USAAEFA PROJECT NO. 76-09-2

LEVEL IV

AD A109515

# ARTIFICIAL ICING TEST

# UTILITY TACTICAL TRANSPORT AIRCRAFT SYSTEM (UTTAS)

# BOEING VERTOL YUH-61A HELICOPTER

FINAL REPORT


JOHN F. HAGEN
MAJ, FA
US ARMY
PROJECT OFFICER/PILOT

EDWARD J. TAVARES
CPT, TC
US ARMY
PROJECT ENGINEER

JAMES C. O'CONNOR
CPT, CE
US ARMY
PROJECT PILOT


JANUARY 1977



DISTRIBUTION STATEMENT A
Approved for public release;
Distribution Unlimited




UNITED STATES ARMY AVIATION ENGINEERING FLIGHT ACTIVITY
EDWARDS AIR FORCE BASE, CALIFORNIA 93523


~~FOR OFFICIAL USE ONLY~~

## DISCLAIMER NOTICE

The findings of this report are not to be construed as an official Department of the Army position unless so designated by other authorized documents.

## DISPOSITION INSTRUCTIONS

Destroy this report when it is no longer needed. Do not return it to the originator.

## TRADE NAMES

The use of trade names in this report does not constitute an official endorsement or approval of the use of the commercial hardware and software.

UNCLASSIFIED

SECURITY CLASSIFICATION OF THIS PAGE (When Data Ent

| REPORT DOCUMENTATION PAGE | | READ INSTRUCTIONS BEFORE COMPLETING FORM |
|---|---|---|
| 1. REPORT NUMBER<br>USAAEFA PROJECT NO. 76-09-2 | 2. GOVT ACCESSION NO.<br>AD-A109515 | 3. RECIPIENT'S CATALOG NUMBER |
| 4. TITLE (and Subtitle)<br>ARTIFICIAL ICING TEST<br>UTILITY TACTICAL TRANSPORT AIRCRAFT SYSTEM (UTTAS)<br>BOEING VERTOL YUH-61A HELICOPTER | | 5. TYPE OF REPORT & PERIOD COVERED<br>FINAL REPORT<br>9 October - 3 November 1976 |
| | | 6. PERFORMING ORG. REPORT NUMBER<br>USAAEFA PROJECT NO. 76-09-2 |
| 7. AUTHOR(s)<br>MAJ JOHN F. HAGEN<br>CPT EDWARD J. TAVARES<br>CPT JAMES C. O'CONNOR | | 8. CONTRACT OR GRANT NUMBER(s) |
| 9. PERFORMING ORGANIZATION NAME AND ADDRESS<br>US ARMY AVIATION ENGINEERING FLIGHT ACTIVITY<br>EDWARDS AIR FORCE BASE, CALIFORNIA 93523 | | 10. PROGRAM ELEMENT, PROJECT, TASK AREA & WORK UNIT NUMBERS<br>68-U-UA-029-01-68-EC |
| 11. CONTROLLING OFFICE NAME AND ADDRESS<br>US ARMY AVIATION ENGINEERING FLIGHT ACTIVITY<br>EDWARDS AIR FORCE BASE, CALIFORNIA 93523 | | 12. REPORT DATE<br>JANUARY 1977 |
| | | 13. NUMBER OF PAGES<br>94 |
| 14. MONITORING AGENCY NAME & ADDRESS(if different from Controlling Office) | | 15. SECURITY CLASS. (of this report)<br>UNCLASSIFIED |
| | | 15a. DECLASSIFICATION/DOWNGRADING SCHEDULE |

16. DISTRIBUTION STATEMENT (of this Report)

DISTRIBUTION STATEMENT A
Approved for public release;
Distribution Unlimited

17. DISTRIBUTION STATEMENT (of the abstract entered in Block 20, if different from Report)

18. SUPPLEMENTARY NOTES

19. KEY WORDS (Continue on reverse side if necessary and identify by block number)

Artificial icing evaluation
Boeing Vertol YUH-61A helicopter
Moderate icing conditions
Deice system functioning and not functioning
Anti-ice systems for engines, engine air induction systems, pitot tubes, and windshields
Electrothermal rotor blade protection

20. ABSTRACT (Continue on reverse side if necessary and identify by block number)

The United States Army Aviation Engineering Flight Activity conducted an in-flight artificial icing evaluation of the ~~Boeing Vertol~~ YUH-61A helicopter equipped with a prototype deice system. This evaluation was conducted from 9 October through 3 November 1976 at Fort Wainwright, Alaska. During the test program 3.2 hours were flown in the artificial icing environment. Of this time, 2.8 hours were flown with the deice system functioning, and 0.4 hour was flown with the system not

(contd)

DD FORM 1 JAN 73 1473 EDITION OF 1 NOV 65 IS OBSOLETE

~~FOR OFFICIAL USE ONLY~~

UNCLASSIFIED

SECURITY CLASSIFICATION OF THIS PAGE (When Data Entered)

20. Abstract

functioning. Anti-ice systems for the engines, engine air induction systems, pitot tubes, and windshields were used during all flights and functioned satisfactorily. With the deice system not functioning, ice accretion on the airframe and flight control surfaces caused significant increases in power required for level flight and significant decreases in autorotational rotor speed with collective full-down. Also noted were increased airframe vibration levels caused by random asymmetrical shedding of ice from the main rotor blades, and damage to the tail rotor blades and transmission fairing caused by ice impact. These adverse results preclude safe operation of the YUH-61A in an icing environment without a main rotor deice system. With the deice system functioning, the YUH-61A successfully flew in artificial icing conditions simulating moderate icing. Three deficiencies were noted which should be corrected prior to flight in icing conditions. These deficiencies are the inability to activate the deice system following an ice detector malfunction; the lack of a system to monitor the integral particle separator turbine operation; and the erratic and unreliable pitot-static indications in level and climbing flight caused by the irregular ice accretion patterns on the lower fuselage nose area. Following correction of these deficiencies the deice system should be tested in natural icing conditions to validate the characteristics observed during this evaluation. In addition to the deficiencies noted, nine shortcomings were identified. Within the scope of this test, the YUH-61A with an anti-ice/deice system displays excellent potential for operating in a moderate icing environment.

**DEPARTMENT OF THE ARMY**
HQ, US ARMY AVIATION RESEARCH AND DEVELOPMENT COMMAND
P O BOX 209, ST. LOUIS, MO 63166

DRDAV-EQ

MAR 7 1978

SUBJECT: USAAEFA Project No. 76-09-2, Artificial Icing Test, Utility Tactical Transport Aircraft System (UTTAS), Boeing Vertol YUH-61A Helicopter, January 1977

SEE DISTRIBUTION

1. The Directorate for Development and Engineering position on USAAEFA's Conclusions and Recommendations are provided herein. Since the UH-61A was not selected for production to meet U.S. Army UTTAS requirements, no action has been taken on this report, however, intended action based on negotiations of the UTTAS Source Selection Evaluation Board (SSEB), had it been selected, are briefly noted. Paragraph numbers from the subject report are provided for reference.

a. Paragraph 62: The test results are clear regarding unsatisfactory operations in moderate icing conditions with the blade deicing system inoperative, however, in the event of failure of the rotor deice system in flight, safe continued operation in trace or light ice may well be possible.

b. Paragraph 65a: Design change to permit the deicing system to operate even after an ice detector malfunction would be included in any future UH-61 procurement efforts.

c. Paragraph 65b:

(1) This paragraph identifies the lack of a system to monitor IPS turbine operation as a deficiency based on:

(a) The engine's susceptibility to FOD without an operable blower.

(b) The requirement to terminate flight in icing conditions if blower was inoperative.

(2) The following points outline our position on why this is not a deficiency:

(a) The requirement for termination of flight if an inoperative blower was indicated was specifically a conservative test requirement and is not considered valid for production considerations.

DRDAV-EQ MAR 7 1978

SUBJECT: USAAEFA Project No. 76-09-2, Artificial Icing Test, Utility Tactical Transport Aircraft System (UTTAS), Boeing Vertol YUH-61A Helicopter, January 1977

(b) No instances of a failed blower of the production configuration has occurred; however, even so, an anti-icing test point was successfully demonstrated with the blower inoperative.

(c) No value of FOD effectiveness with or without a failed blower is known; however, experience with ice ingestion indicated no sizable piece could get through the swirl vanes, past the splitter lip, through the deswirl vanes and IGV without being broken up.

(d) Instances of FOD encountered thus far, blower operative, did not disable an engine beyond some reduced power. The conclusion noted in paragraph 65.b will be part of a continuing evaluation, but is not considered imperative until conditions warrant it.

(e) Production maintenance inspections procedures are being established which will include at least a borescope port on the blower.

d. Paragraph 65c: Correction would be incorporated for future utilization of the UH-61.

e. Paragraph 66a thru d and f thru i: Correction to these shortcomings were negotiated by the UTTAS SSEB to be included in UH-61 production specifications.

f. Paragraph 66e: We do not agree that this is a shortcoming. Center windshield ice protection was deliberately deleted because no adverse impact from its non-existence on the CH-47 and S-61 helicopters. The increased visibility, if ice protection were present, is insignificant in relation to its cost, due to the large offset angle of each crewmember.

g Paragraphs 69 thru 72 and 74 thru 77: Concur with these recommendations, action would be taken if future utilization of the UH-61 is required.

h. Paragraph 73: This WARNING has a significant drawback since the purpose of the helicopter is troop assault in which rapid unloading is essential, therefore, it would be applied to peacetime operation only as a CAUTION.

2. This report is another documented example of how essential rotor system deicing systems are for adequate airworthiness when operation in moderate ice is required.

FOR THE COMMANDER:

Walter A. Ratcliff

WALTER A. RATCLIFF
Colonel, GS
Director of Development
and Engineering

# PREFACE

The artificial icing test of the YUH-61A helicopter was conducted jointly by the United States Army Aviation Engineering Flight Activity (USAAEFA) and Boeing Vertol Company at Fort Wainwright, Alaska. The test aircraft was maintained by USAAEFA with backup support provided by Boeing Vertol. Aircraft test instrumentation was supplied, installed, and maintained by Boeing Vertol personnel.

Special acknowledgment is made for the outstanding assistance and support provided at Fort Wainwright by MAJ James C. Hoodenpyle, CW2 Jefferson R. Watts, and the officers and men of the 222d Aviation Battalion.

Descriptive material on the Normalair-Garrett ice detector system presented in appendix D is used with permission of the company.

# TABLE OF CONTENTS

Page

INTRODUCTION

Background . . . . . 3
Test Objectives . . . . . 3
Description . . . . . 4
Test Scope . . . . . 4
Test Methodology . . . . . 6

RESULTS AND DISCUSSION

General . . . . . 7
Deice System Operation . . . . . 7
Anti-Ice and Heating Systems Operation . . . . . 9
General . . . . . 9
Engine Anti-ice . . . . . 9
Engine Air Induction Anti-Ice . . . . . 10
Engine Inlet (D-ring) Fairing . . . . . 10
Engine Transmission Fairing . . . . . 10
Windshield Anti-Ice . . . . . 10
Pitot-Static Anti-Ice . . . . . 11
Cabin Heater . . . . . 12
Integral Particle Separator . . . . . 12
Flight Control Surface Ice Accretion and Shedding Characteristics . . . . . 12
General . . . . . 12
Unheated Blade Phase . . . . . 13
Heated Blade Phase . . . . . 15
Airframe Ice Accretion and Shedding Characteristics . . . . . 17
Level Flight Performance . . . . . 20
Autorotational Performance . . . . . 22
Handling Qualities . . . . . 22
Vibration Characteristics . . . . . 24
Human Factors . . . . . 24
Ice Detectors . . . . . 25
General . . . . . 25
Rosemount Ice Detector . . . . . 25
Normalair-Garrett Ice Detector . . . . . 26

Page

CONCLUSIONS

General . . . . . . . . . . . . . . . . . . . . . . . . . . . 27
Deficiencies and Shortcomings . . . . . . . . . . . . . . . . 28

RECOMMENDATIONS . . . . . . . . . . . . . . . . . . . . . . . . 30

APPENDIXES

A. References . . . . . . . . . . . . . . . . . . . . . . . . 31
B. Deice/Anti-Ice Systems Description . . . . . . . . . . . . 33
C. Helicopter Icing Spray System Description . . . . . . . . . 46
D. Instrumentation and Special Equipment . . . . . . . . . . . 48
E. Test Techniques and Data Analysis Methods . . . . . . . . . 61
F. Icing Flight Summaries . . . . . . . . . . . . . . . . . . 72
G. Test Data . . . . . . . . . . . . . . . . . . . . . . . . . 82
H. Photographs . . . . . . . . . . . . . . . . . . . . . . . . 85

DISTRIBUTION

# INTRODUCTION

## BACKGROUND

1. The United States Army requires an improved operational capability in its utility transport aircraft to satisfy the demand for increased performance and survivability in the mid-intensity combat environment. The utility tactical transport aircraft system (UTTAS) is being developed in response to this requirement and will replace the current utility helicopter in the Army inventory. On 30 August 1972 the United States Army Aviation Systems Command (AVSCOM)* awarded a contract to the Boeing Vertol Company to produce three prototype aircraft and one ground test vehicle. The United States Army Aviation Engineering Flight Activity (USAAEFA) completed an Army Preliminary Evaluation of the Boeing YUH-61A in March 1976. A Government Competitive Test (GCT) was completed in September 1976.

2. The UTTAS shall be capable of operation under climatic conditions up to and including moderate icing (ref 1, app A). As a result, USAAEFA was tasked by an AVSCOM test directive (ref 2) to conduct artificial icing tests of the YUH-61A in accordance with the approved test plan (ref 3).

## TEST OBJECTIVES

3. The overall objectives of the UTTAS artificial icing tests were as follows:

a. To provide data to be used for evaluating the ability of the helicopter to effectively operate in a moderate icing environment.

b. To detect, and allow for early correction of, any aircraft deficiencies or shortcomings.

4. Specific objectives of each testing phase are listed below.

a. Unheated blade phase:

(1) Evaluate the effectiveness of the windshield, pitot-static, engine air induction, and engine anti-ice systems.

(2) Determine the need for additional anti-ice/deice systems.

b. Heated blade phase:

(1) Determine the potential effectiveness of the contractor-provided prototype anti-ice/deice systems.

*Since redesignated the Army Aviation Research and Development Command (AVRADCOM).

(2) Provide the UTTAS competitors a limited opportunity to further develop anti-ice/deice systems.

## DESCRIPTION

5. The UTTAS is a twin-turbine, single-main-rotor helicopter designed for transporting cargo, 11 combat troops, and weapons during visual or instrument meteorological conditions (VMC or IMC). Nonretractable wheel-type landing gear are provided. The main and tail rotors are both four-bladed, with a capability of manual main rotor blade and tail pylon folding. A movable horizontal stabilizer is located on the tail rotor pylon. A more detailed description of the YUH-61A (SN 73-21658) is contained in the prime item development specification (PIDS), operator's manual, and the GCT final report (refs 4, 5, and 6, app A). The prototype deice system installed on the YUH-61A is designed to provide the capability to deice the main rotor blades, tail rotor blades, and horizontal stabilizer. The system incorporates electrothermal heating elements installed on the leading edges of the main and tail rotor blades and the horizontal stabilizer. The heating elements on the main and tail rotor blades are an integral component of the standard manufactured blades and were not a kit component installed specifically for the icing test. With the exception of one main rotor blade, the blades had been installed and flown on test aircraft prior to the icing tests. When the deice system is turned on, its operation is controlled by a deice controller unit based on signals received from an ice detector and outside air temperature (OAT) sensor. System ON time is varied as a function of OAT and system OFF time is varied as a function of icing rate. The YUH-61A also has anti-ice provisions for the pilot and copilot windshields, pitot tube, engine, engine inlet fairing, and engine transmission fairing. A detailed description of the YUH-61A deice and anti-ice systems is presented in appendix B. A description of the helicopter icing spray system (HISS) installed on a CH-47C helicopter (SN 68-15814) is presented in appendix C and in references 7 and 8, appendix A.

## TEST SCOPE

6. In-flight artificial icing, utilizing the HISS, was conducted in the vicinity of Fort Wainwright, Alaska, from 9 October through 3 November 1976. A total of 9 icing flights were conducted in 10.6 flight hours, of which 3.2 hours were in the artificial icing environment. The aircraft was iced at test conditions presented in table 1. Icing summaries for each flight are presented in appendix F. Flight limitations contained in the operator's manual and the safety-of-flight release (refs 9 and 10, app A) were observed during the testing.

Table 1. Icing Test Conditions.[1]

| Flight Number[2] | Average Static Outside Air Temperature (°C) | Programmed Liquid Water Content ($gm/m^3$) | Time in Icing Condition (min) | Average Density Altitude (ft) | Average True Airspeed (kt) | Average Gross Weight[3] (lb) | Average Center of Gravity[3] (in.) |
|---|---|---|---|---|---|---|---|
| 2[4] | -6.5 | 0.25 | 7 | 1590 | 86 | 15,580 | 205.6 |
| 4 | -11.5 | 0.25 | 10 | 80 | 88 | 15,860 | 206.8 |
| 5 | -6.5 | 0.50 | 22 | 2940 | 84 | 15,800 | 206.5 |
| 6 | -11.0 | 0.25 | 39 | 6680 | 91 | 15,760 | 206.3 |
| 7 | -6.0 | 0.75 | 13 | 6140 | 92 | 15,740 | 206.2 |
| 9 | -16.5 | 0.25 | 48 | -1100 | 91 | 15,640 | 205.8 |
| 10 | -13.0 | 0.50 | 29 | 1560 | 89 | 15,720 | 206.2 |
| 11[5] | -12.5 | 0.25 | 6 | -100 | 91 | 15,980 | 207.3 |
| 12[5] | -13.5 | 0.25 | 18 | -400 | 90 | 15,860 | 206.8 |

[1]Normal utility configuration. Rotor speed: 286 rpm (100 percent).
[2]Nonicing flights are not presented.
[3]Average values excluding effects of accreted ice.
[4]Deice system ice detector malfunction.
[5]Unheated phase. Main rotor, tail rotor, and horizontal stabilizer deice OFF.

## TEST METHODOLOGY

7. Artificial icing of the YUH-61A was conducted by flying the test aircraft in a spray cloud generated by the HISS. A detailed discussion of the test sequence and procedures is contained in reference 3, appendix A. Prior to entering the cloud, the test aircraft was stabilized at the predetermined test conditions and base-line trim data were recorded. The test aircraft was then immersed in the spray cloud. After ice accumulation the test aircraft was again stabilized outside the spray cloud at the initial trim airspeed and another data record taken. The ice accretion was then documented by photographic and visual observation. Following data recording, a steady-state autorotation was performed to determine rotor speed degradation with ice accretion. Immersion times were based on pilot judgment, system operation, power required, vibration, visual observations, duration of the HISS water supply, and prior test results.

8. A detailed description of test instrumentation and special equipment installed on the test aircraft is presented in appendix D. In addition to the Rosemount ice detector integral to the deice system (app B), additional systems manufactured by Rosemount Engineering Company and Normalair-Garrett Ltd, and a USAAEFA-designed and fabricated visual probe were installed to measure ice severity and accretion. Brief descriptions of the Rosemount and Garrett systems are presented in appendix D and a detailed discussion can be found in references 11 and 12, appendix A. The USAAEFA visual ice accretion probe is discussed in paragraph 18, appendix D, and shown in photo 6, appendix D.

9. Test techniques and data analysis methods are presented in appendix E. A Handling Qualities Rating Scale (HQRS), the methods used to determine HISS spray cloud parameters, and definitions of icing types and severities are also presented in appendix E.

# RESULTS AND DISCUSSION

## GENERAL

10. An in-flight artificial icing evaluation of the YUH-61A was conducted to determine the capability of the aircraft to fly in icing conditions without a deice system and to determine the potential effectiveness of the contractor-provided deice system. The effectiveness of the windshield, pitot-static, engine, and engine air induction anti-ice systems was also evaluated. The ice accretion and shedding characteristics of the YUH-61A airframe and flight control surfaces were documented. The capabilities of two special equipment ice detectors to detect and measure icing conditions were evaluated. Ice accretion on the airframe and flight control surfaces during the unheated blade phase caused significant increases in power required for level flight and significant decreases in autorotational rotor speed with collective full-down. Additionally, random asymmetrical shedding of ice from the main rotor blades caused increased airframe vibration levels and there was damage from ice impact on the tail rotor gearbox fairing and tail rotor blades. The aircraft does not possess the capability to safely operate in an icing environment without a main rotor deice system. With the deicing system functioning, the YUH-61A successfully flew in artificial icing conditions for periods of time up to 48 minutes, and displays excellent potential for operating in a moderate icing condition. Three deficiencies were noted which should be corrected prior to flight in icing conditions. These deficiencies are the inability to activate the deice system following an ice detector malfunction; the lack of a system to monitor the integral particle separator (IPS) turbine operation; and the erratic and unreliable pitot-static indications in level and climbing flight caused by the irregular ice accretion patterns on the lower front fuselage area. Nine shortcomings which degraded crew or aircraft operation were noted. Following correction of the three deficiencies, testing of the deice system in natural icing conditions should be conducted to validate the ice accretion and shedding characteristics and aircraft performance characteristics observed during this evaluation.

## DEICE SYSTEM OPERATION

11. The YUH-61A deice system was evaluated for operational characteristics, electrical switching transients, and electrical power requirements during the heated blade phase. During 2.8 hours of flight time in the artificial icing environment, the deice system automatically cycled 58 times with only two malfunctions. A system cycle consisted of four ice accretion signals from the ice detector, followed by twelve electrical power pulses distributed to the deice system heating blankets. The only component change was the deice system ice detector, which malfunctioned during the first icing flight (para 12). One automatic system shutdown, initiated by the system fault detection circuitry, occurred (para 13). The heating blankets

on the main and tail rotor blades were installed during the construction of the blades. These blankets required no maintenance, although the main rotor blades had accumulated 163, 115, 21, and zero hours, respectively, and the tail rotor blades had accumulated 409, 409, 210, and 210 hours, respectively, prior to the icing tests.

12. Automatic cycling of the deice system was accomplished by the deice controller, which received an icing signal (pulse) from the system ice detector. The pulse signals were sent from the ice detector when a predetermined thickness of ice was accumulated. The ice detector probe was then readied for another ice accumulation (icing signal) by electrically heating the probe and shedding the ice. During the first icing flight, ice continuously accumulated on the probe due to a failure of the probe heating element. Therefore, the ice detector was unable to send repeated icing signals to the deice controller as required for system operation. The system incorporated no provisions to automatically or manually activate the system if the ice detector malfunctioned. Failure of the ice detector heating circuit renders the deice system inoperable. The inability to activate the deice system following an ice detector malfunction is a deficiency.

13. As discussed in the system description in appendix B, the deice system contains fault detection logic which deactivates the system and illuminates the ROTOR DEICE caution panel light on the annunciator panel when a fault is detected. One incident of this light illuminating occurred after a cloud immersion of 30 minutes at -16.5°C and a liquid water content (LWC) of 0.25 grams per cubic meter (gm/m$^3$). The aircraft immediately exited the cloud and the deice system ROTOR/STAB switch was cycled OFF and ON. The caution light extinguished and the aircraft reentered the icing environment for an additional 18 minutes (three system cycles) without further incident. The failure could not be duplicated and did not occur during the remaining tests. Postflight inspection of the system and analysis of the available data indicated an electrical power transient was the probable cause for the momentary system failure. An investigation should be conducted by Boeing Vertol to determine the cause of the illumination of the ROTOR DEICE caution light.

14. Engagements and disengagements of the rotor deice system were conducted to evaluate the effects of electrical switching transients. The tests were accomplished on the ground and in flight with all anti-ice systems and both stability and control augmentation systems (SCAS) ON. When the ROTOR/STAB switch was placed ON or OFF, the vertical situation indicator exhibited a rapid ±3-degree transient roll attitude oscillation and a ±150-foot transient oscillation was observed on the radar altimeter needle. Both indicators returned to their original position following the momentary oscillation with no input to SCAS or airframe. Placing the deice ROTOR/STAB switch ON or OFF while on the ground at 100 percent rotor speed resulted in a mild transient airframe vertical response. This response required no pilot compensation or reaction. In flight, no airframe or SCAS response was observed following a deice system engagement or disengagement. No other system

interference problems were observed with operation of the deice system. The mild switching transients when the deice system is engaged or disengaged are a shortcoming.

15. The electrical power requirements of the deice system were monitored in flight using the generator load meters and were calculated from recorded data following each flight. The electrical power required to operate the main rotor blades ranged from 19.1 to 20.3 kilovolt-amperes (KVA). The electrical power required for the tail rotor was 8 to 8.5 KVA and 11.4 to 12 KVA for the horizontal stabilizer. Since electrical power was not sent simultaneously to the main and tail rotors and the horizontal stabilizer, the maximum load to operate the deice system was 20.3 KVA. This electrical power requirement was 50 percent of the maximum continuous generator rating (41 KVA) of a single generator and closely approximated the Boeing Vertol pretest estimate of 20.7 KVA. Within the scope of this test, the electrical power requirements of the deice system were satisfactory.

16. The electrical power pulse duration during each cycle of the deice system was measured from recorded data. The pulse duration was automatically varied by the deice controller as a function of total air temperature and varied from 3.6 seconds at -5°C to 11 seconds at -15°C. The variation of pulse duration observed was in agreement with Boeing Vertol pretest estimates. No adjustment to the pulse duration was required during this evaluation, since control of heated surface ice accretion and shedding on the main rotor blade was satisfactory (paras 34 and 36).

## ANTI-ICE AND HEATING SYSTEMS OPERATION

### General

17. Throughout the tests the anti-ice systems, cabin heating, and associated subsystems were continuously evaluated. The operating characteristics of these systems were the same for both the heated and unheated phases.

### Engine Anti-Ice

18. Engine anti-icing was accomplished by a combination of hot axial compressor discharge air and heat transfer from the air/oil cooler in the engine frame. Operation of the system was controlled by the ENG INLET switch located on the overhead switch panel. A detailed discussion of the system is presented in appendix B. During both phases of testing the system operated without any failures and with no unscheduled maintenance being required. Within the scope of this test, the engine anti-ice system is satisfactory.

## Engine Air Induction Anti-ice

### Engine Inlet (D-ring) Fairing:

19. The engine inlet (D-ring) was heated by hot engine bleed air. A system description is presented in appendix B. The system operated with no failures and no ice accumulation was observed on the inlets. Ice was accreted on the top portion of the engine nacelle just aft of the D-ring (photo 1, app H). However, no shedding of this ice was observed. Within the scope of this test, operation of the engine inlet anti-ice system is satisfactory.

### Engine Transmission Fairing:

20. The engine transmission fairings were electrically heated and activated by the ENG INLET switch on the overhead switch panel. The system is discussed in appendix B. The system operated satisfactorily during this evaluation, with no failures or unscheduled maintenance being required. One occurrence of ice accumulation on the heated surfaces was observed. At a test condition of -13°C and 0.50 $gm/m^3$ LWC, a small amount of ice (1-inch diameter) was accreted on the right fairing. The area was inadequately heated due to an instrumentation wire interference. The wire arrangement was corrected and no further ice accumulation was observed. Within the scope of this test, the engine transmission fairing anti-ice system is satisfactory.

21. Installation of the heated engine transmission fairings required that the oil filler caps be modified to ensure proper seating of the fairings. Due to the electrical heating elements on the inside of the fairings, inadequate clearance existed between the fairings and the filler caps. The filler caps were filed until the fairings would seat properly. The insufficient clearance between the heated engine transmission fairings and the engine transmission oil filler caps is a shortcoming.

22. The engine transmission oil sight gauges are located on the forward edge of each transmission. The fairings used during the GCT were nonheated and had a cut-out in the fairing to view the oil sight gauge. To prevent ice accumulation on the sight gauge, the cut-out was eliminated on the heated fairings. To check the oil level, the heated dome-shaped fairing had to be removed. The inconvenience associated with removal of the fairings inhibits the required preflight check of the engine transmission oil level. The inaccessibility of the engine transmission oil sight gauge with the heated fairings installed is a shortcoming.

## Windshield Anti-Ice

23. The pilot and copilot windshields are electrically heated and controlled by individual switches on the overhead switch panel. A detailed discussion of the system is presented in appendix B. The windshield anti-ice system was activated for all cloud immersions and operated with no failures. The heated portion of the windshields remained clear of ice during all cloud immersions. Ice accumulation was observed around the upper and outboard windshield mounting supports

(photo 2, app H). These buildups were caused by ice accretion on the windshield mounting bolt heads. The ice thickness and area covered was a function of temperature, LWC, and time in the cloud. The maximum thickness observed was 3 inches following a 20-minute immersion at -13°C and 0.5 gm/m$^3$ LWC. The ice growth pattern was from the mounting bolts toward the center of the windshield. No interference between the accreted ice and the windshield wipers was observed. No interior fogging of the windshields occurred, although intentional cold soaking of the aircraft was not accomplished. Activation of the windshield anti-ice caused no observed heading change on the magnetic compass. Within the scope of this test, the pilot and copilot windshield anti-ice system is satisfactory. The exterior protuberances around the pilot and copilot windshields should be minimized to reduce ice accretion.

24. The center windshield has no ice protection and iced over immediately upon entering the spray cloud. Ice thickness measurements for the individual icing sorties are recorded in the icing flight summaries presented in appendix F. The pilot and copilot field of view is restricted after an icing encounter and would hamper the crew's ability to visually acquire the runway environment after breaking clear of clouds during an instrument approach. Additionally, circling instrument approaches will be more difficult to execute when combining the restricted field of view with reduced visibility. Tactical operations that require flight in icing conditions, an instrument approach, and then nap-of-the-earth (NOE) flight to a landing zone will be difficult to execute. The lack of ice protection on the center windshield is a shortcoming.

25. Operation of the windshield wipers was necessary while in the spray cloud to provide a clear view of the spray aircraft. The wipers were activated as the aircraft entered the cloud. Starting the wipers after ice had been accreted on the wiper arms was not accomplished. The two-speed capability of the wipers provided adequate moisture removal at all test conditions and they operated with no failures. No scratching of the exterior glass was observed. In one case after exiting the spray cloud, a failure of the wipers to properly park occurred. The wiper motor lacked sufficient power to move the wiper across the dry glass surface. The unparked wipers obscured forward vision and were distracting. The failure of the windshield wipers to return to the PARK position on a dry windshield is a shortcoming.

**Pitot-Static Anti-Ice**

26. The pitot-static system had two pitot tubes located on the lower nose area and two static ports located on the left and right sides of the fuselage aft of the cockpit doors. The pitot tubes were electrically heated and the static ports were unheated. No ice accretion was observed on the forward portion of the pitot tubes and the system operated with no failures. Although the static ports were unheated, no ice accumulation was observed. Within the scope of this test, the pitot-static anti-ice system is satisfactory.

27. Ice accretion was observed on the unheated pitot tube support struts (photo 3, app H). This ice buildup did not mask the pitot tube inlet orifice and did not cause any apparent change in indicated airspeed. A maximum ice thickness of 1.1 inches on the struts was observed following a 29-minute immersion at -13°C and 0.5 $gm/m^3$ LWC. Although this buildup did not extend forward of the 3.25-inch length of the pitot tube, larger ice buildups during increased periods of immersion could affect indicated airspeed accuracy and may finally result in pitot tube blockage. Ice protection should be provided for the pitot tube support strut.

### Cabin Heater

28. Cabin heating was provided by mixing engine compressor bleed air and outside air and then ducting the air to the cockpit and cabin areas. The system was controlled by a switch and temperature rheostat located on the overhead switch panel. A detailed discussion of the heating system is contained in reference 5, appendix A. At OAT's as low as -16.5°C, a comfortable cabin temperature was maintained with the rheostat set at approximately 50 percent. No interior fogging of the heated windshields or windows was observed, although relative humidity levels observed were low. Within the scope of this test, the cabin heating system operated satisfactorily at OAT's down to -16.5°C.

## INTEGRAL PARTICLE SEPARATOR

29. An IPS on each engine is designed to protect the engine from foreign object damage (FOD) (ref 5, app A). Without an operable IPS the engine is very susceptible to FOD, especially in an icing environment. Failure of either IPS during the icing tests would have required termination of flight in icing conditions. For this reason, a special IPS pressure gauge was installed in the cockpit to monitor IPS operation. The production aircraft does not incorporate a system to monitor IPS operation. The lack of a system to monitor IPS turbine operation is a deficiency.

## FLIGHT CONTROL SURFACE ICE ACCRETION AND SHEDDING CHARACTERISTICS

### General

30. Ice accretion and shedding characteristics of the main and tail rotor blades and horizontal stabilizer surfaces were documented by in-flight visual observation, high-speed photography, and postflight measurements. The effects of ice accretion on handling qualities were quantitatively and qualitatively evaluated following spray cloud immersion (para 52). The changes in level flight and autorotational performance with ice accretion are discussed in paragraphs 45 through 51. Significant differences in the accretion and shedding characteristics were noted between the heated blade phase and unheated blade phase, and each phase will be discussed separately. An ice accretion pattern called pebbling was observed on

the lower chord of the main rotor blades during both testing phases. Pebbling was characterized by small, irregularly spaced ice particles accreting on the blade surface (photo 4, app H).

31. No significant ice accretion was observed on the tail rotor blades and hub during either test phase. Factors which may have contributed to this lack of ice accretion were warm engine exhaust air bathing the tail rotor, shallow depth of the spray cloud, and downwash effects of the main rotor disc on the cloud, which reduced the exposure of the tail rotor to the cloud.

## Unheated Blade Phase

32. To determine ice accretion and shedding characteristics of the main rotor and tail rotor blades and the horizontal stabilizer, the deice systems were not activated during the unheated blade phase. The test technique consisted of two separate cloud immersions. The first immersion was conducted at a test condition of -12.5°C and 0.25 $gm/m^3$ LWC and was terminated when the visual probe accreted 1/4 inch of ice. Following the first immersion, ice accretion on the main rotor blade and horizontal stabilizer was slight. Increases in power required for level flight (para 47) and autorotational rate of descent (para 51) were observed but did not limit test procedures. Vibration changes or aircraft damage caused by ice shedding were not observed. The second immersion was conducted at a test condition of -13.5°C and 0.25 $gm/m^3$ LWC and was terminated when the visual probe accreted 1/2 inch of ice. Following the second immersion, ice accretion on the main rotor blade leading edge extended from blade station 72 (24 percent radius) to approximately blade station 182 (62 percent radius) (photo A). The thickness of this ice varied from 1/2 to 7/8 inch. On the main blade upper surfaces, the ice accretion extended 4 inches aft from the leading edge at blade station 72 (24 percent radius), gradually tapering to zero at approximately blade station 182 (62 percent radius). This ice was very irregular and rough, and varied from 1/2 to 5/8 inch thick. On the main blade lower surfaces, pebbling extended full chord aft from the leading edge between blade stations 72 (24 percent radius) and 130 (44 percent radius), and then tapered to zero at approximately blade station 182 (62 percent radius). Significant changes in level flight performance (para 47) and autorotational descent performance (para 51) were observed. Ice shedding also caused a change in vibration characteristics (para 53) and airframe damage (para 33). During this immersion, ice accreted on the leading edge of the left and right horizontal stabilizer between approximately 50 percent span and the outboard tips. Chordwise accretion was zero at mid span and tapered to 8 inches aft at the outboard tips on both upper and lower surfaces. The thickness of the leading edge ice varied from 3/32 inch at mid span to 1/4 inch at the tips. No significant ice accretion was observed on the tail rotor during either immersion.

33. Random main rotor blade ice shedding was observed throughout the unheated blade phase. No ice shedding from the horizontal stabilizer was observed. Three incidents of asymmetrical shedding from the main rotor blades occurred during the second flight of the unheated blade phase. Each occurrence was characterized by a moderate lateral airframe vibration (para 53) which lasted approximately

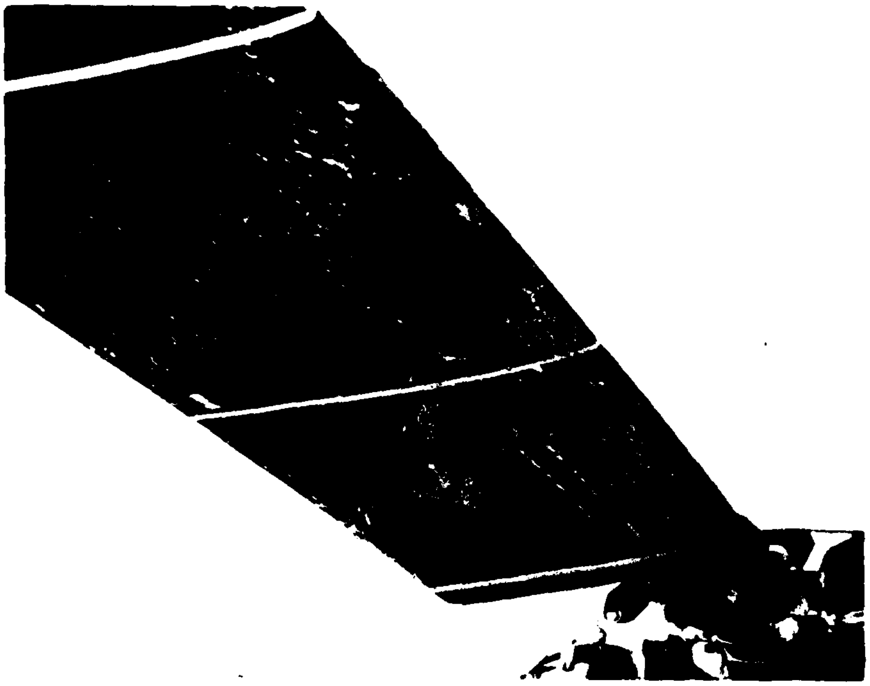

Photo A. Main Rotor Blade Lower Chord - Unheated Phase.

1 minute. Flight control inputs by the pilot were not required to maintain adequate aircraft control during the asymmetrical sheds (HQRS 2). During landing and engine shutdown following this flight, numerous ice particles were observed shedding from the main rotor blades. The ice was shed in all directions and presented a potential hazard to ground personnel in the vicinity of the helicopter. The WARNING shown below should be placed in the operator's manual. Damage to the tail rotor gearbox fairing on the vertical fin was observed following this flight. Ice particles also impacted on the tail rotor blades, causing three blade skin deformations. The tail rotor blade strikes did not require blade replacement.

**WARNING**

> Following flight into icing conditions, ice shed from the rotor blades and/or other rotating components presents a hazard to personnel during ground operation and shutdown of the helicopter. Ground personnel should remain well clear of the helicopter during landing, ground operation, and shutdown. Passengers/crewmembers should not exit the helicopter until the rotor has stopped.

## Heated Blade Phase

34. The ice accretion and shedding characteristics of the main and tail rotor blades and horizontal stabilizer control surfaces were evaluated with the deice system activated. The deice system was activated prior to entering the spray cloud and cycled automatically based on ambient temperature and icing severity. A characteristic heated blade ice accretion pattern is shown in photo B. The heated surfaces of the main rotor blades accumulated ice only at conditions of -16.5°C and 0.25 gm/m$^3$ LWC. This ice was 1/4 inch wide by 1/8 inch thick and was observed on the leading edge from blade station 116 (39 percent radius) to blade station 161 (55 percent radius). Main rotor blade internal counterweights are located behind the leading edge at the same blade stations. Apparently these weights were a sufficient heat sink to allow accretion of the leading edge ice. Also, a trace of upper surface icing was observed at the same test conditions. The ice accretion pattern on the unheated lower blade surfaces was similar to the accumulations observed during the unheated tests. No run-back and refreezing of moisture from the heated surfaces of the main rotor blades was found during the testing.

35. Ice accumulations on the heated surface of the horizontal stabilizer were observed at ambient temperatures less than -11°C. The buildups occurred along the outboard 50 percent of the aft edge of the deice boot upper and lower surfaces. The maximum thickness measured was 1/2 inch, tapering to zero at 50 percent span. It appeared that the melted ice had run back to the trailing edge of the deice boot and refrozen. Heated surface icing also occurred at test conditions of -13°C and 0.50 gm/m$^3$ LWC. A 1/2-inch thick accumulation was observed covering the outboard 10 percent of the leading edge (photo 5, app H). At these test conditions the heating capacity of the surface was inadequate and is a shortcoming.

Photo B. Main Rotor Blade Lower Chord - Heated Phase.

36. Ice shedding during cycling of the deice system caused no observed changes in handling qualities, vibration characteristics, or power management. The ice particles shed from the heated surfaces were observed to be extremely small and presented no FOD hazard to the engines, airframe, or rotating flight control surfaces.

## AIRFRAME ICE ACCRETION AND SHEDDING CHARACTERISTICS

37. Airframe ice accretion and shedding characteristics were documented by in-flight visual observation, high-speed photography, and postflight measurements. The effects of ice accumulation on handling qualities were quantitatively and qualitatively evaluated (para 52). The changes in level flight and autorotational performance with ice accretion are discussed in paragraphs 45 through 51. The same airframe accretion and shedding characteristics were noted during both the heated and unheated blade phases.

38. The majority of the ice accreted on the airframe occurred in the forward fuselage area. Negligible ice was accreted on the fuselage sides, fuselage bottom, upper fuselage (except the forward crown), engine nacelles, and tail boom. There were two types of glime ice accretion patterns (characteristics) observed. The ice accretion pattern at temperatures warmer than -16.5°C was characterized by a rough surface with numerous irregularities (photo C). As the time in the cloud was increased, these irregularities grew in size, forming vertical columns of ice which grouped together to create ice ridges. The ice ridges were most pronounced on the chin bubbles, lower nose area, and pilot foot-steps. The second distinctive pattern was the ice formation at a temperature of -16.5°C, which was characterized by a generally smooth uniform surface with no ice ridge formations (photo D). The ice particles on the fuselage were smaller and more numerous, which created the smoother, more regular-textured surface.

39. Following an immersion of 29 minutes at -13°C and 0.50 $gm/m^3$ LWC, erratic and erroneous ship's system pitot-static indications were observed in level and climbing flight. The first indication of a pitot-static system error was noted during the postcloud level flight performance test. Random airspeed fluctuations of ± 1 to 3 knots were observed on the pilot sensitive airspeed indicator. These airspeed changes were not seen on the copilot production-type indicator. After the level flight performance data were obtained, a climb was initiated at 90 knots indicated airspeed (KIAS) to gain altitude to conduct the autorotational performance tests. As the rate of climb increased to 800 feet per minute (ft/min), the indicated airspeed decreased to approximately 60 KIAS in a level pitch attitude. At a rate of climb of 1000 ft/min, indicated airspeed rapidly decreased to zero. This erroneous airspeed information was received by the SCAS and resulted in an increase in the horizontal stabilizer incidence angle. This caused the aircraft to pitch down and required an aft longitudinal input of approximately 0.5 inch to maintain a level pitch attitude (HQRS 7). Cruise guide indicator readings of 100 and 130 percent were observed at rates of climb of 800 and 1000 ft/min, respectively.

Photo C. Typical Accretion Pattern at Temperatures Warmer than -16.5°C.

Photo D. Typical Accretion Pattern at 16.5°C.

The pitot-static errors were caused by the thick and irregularly shaped ice accumulations on the fuselage nose and chin bubbles (photo 6, app H). The ice accretion pattern on the lower portion of the nose was very irregular, with numerous localized buildups of 3 inches. Ice accumulations of 1-5/8 inches were measured on the chin bubbles in a position which influenced airflow to the pitot tubes in level and climbing flight. The pitot-static system appeared to operate satisfactorily during descents and autorotation. This further indicated that the pitot-static errors were caused by the irregular, rough ice surfaces forward of the pitot tubes. Pitot-static errors were not observed during climbs with less ice accretion on the forward fuselage area. The erratic and unreliable pitot-static indications in level and climbing flight caused by the irregular ice accretion pattern on the lower fuselage nose area are a deficiency.

40. Airframe ice accretion aft of the windshield and fuselage nose areas was generally limited to fuselage protuberances such as handholds, rivet heads, foot-steps, etc. All side and overhead windows remained clear of ice. An insignificant amount of ice accretion was observed on the right side of the tail boom aft of the avionics access door. Ice accumulated on the cabin heater inlet located on the forward crown and is discussed in paragraph 41. A maximum of 1-1/2 inches of ice was observed on the forward crown side work platform supports located directly in front of the engines. One incident of ice shedding from a support and entering the engine inlet was observed. Postflight inspection of the engine and particle separator turbine showed no damage. Ice accumulation was also observed on the fixed upper handholds located in front of the work platform supports. No ice shedding was observed from these handholds. Elimination of ice accretion on these protuberances would decrease the possibility of engine ice ingestion. The forward crown side work platform supports and upper handholds should be redesigned to reduce ice accretion.

41. The cabin heating system receives outside air for mixing with hot engine bleed air through a circular screened inlet located on the right side of the forward crown. Following a 39-minute flight at -11°C and 0.25 gm/m$^3$ LWC, approximately 90 percent of the heater inlet screen became blocked with ice. No noticeable degradation in cabin heating was observed with the inlet blocked. The ambient air necessary for proper operation could have entered the heater mixer unit through the 1/4-inch gap between the forward crown inlet screen and the mixer unit inlet duct. To preclude automatic shutdown of the cabin heater due to overheating in the mixing unit, an air deflector was fabricated and installed in front of the heater inlet. This deflector kept at least 50 percent of the heater inlet free of ice accretion on subsequent flights. The ice accretion on the cabin heater air inlet on the right forward crown area is a shortcoming.

42. Another area which accreted ice was the upper fuselage skin directly forward of the engine inlets. This area contained numerous rivet heads and screw heads which accreted ice on all flights (photo 7, app H). Ice accumulations of 1/2 to 3/4 inch were also observed between the No. 2 engine transmission fairing and fuselage skin. Although no shedding from these areas was observed, the fuselage

skin protuberances forward of the engine inlets should be reduced to decrease the likelihood of ice ingestion by the engine.

43. Operation of the unheated ship's OAT probe was evaluated prior to and during cloud immersion. Maximum ice accumulations of 1-3/4 inches were observed covering 75 percent of the probe surface. No degradation in the OAT probe performance was noted with ice accretion. Within the scope of this test, the ship's standard OAT probe is satisfactory for use in an icing environment.

44. Minimal ice shedding was observed from ice accumulations on the airframe. Generally, ice which shed from the nose area below the windshields departed the airframe outboard and down, away from the aircraft. Numerous ice sheddings from the windshield wiper arms did occur. These particles ranged in size from 1/2 to 1-1/2 inches in diameter. The trajectory was normally outboard and aft along the fuselage below the engine inlets. One incident of center windshield shedding was observed when the aircraft descended into warmer temperatures. A piece of approximately 3/4 square foot in area departed upward and impacted with the main rotor blades. There was no blade damage and no engine ice ingestion was observed.

## LEVEL FLIGHT PERFORMANCE

45. Level flight performance data were obtained during both test phases to determine the change in engine power required with airframe and flight control surface ice accretion. The tests for each phase were conducted at the test conditions shown in table 1. Data were first obtained prior to entering the icing environment and again after exiting the spray cloud. A summary of the level flight performance results for both test phases is presented in table 2

46. During the heated blade phase an increase in engine shaft horsepower (shp) required with ice accretion was noted. The changes in power required were a function of time in the icing environment, ambient temperature, programmed LWC, and change in gross weight due to fuel burnoff and ice accretion. At no time during the testing did the power required to safely operate in an icing environment with all deice/anti-ice systems operating become a limiting factor. However, the level flight performance data show that even with a functioning deice system a degradation in range and endurance can be expected. Within the scope of this test, a quantitative level flight performance assessment was not made.

47. During the unheated blade phase, significant power-required increases with ice accretion were noted. A comparison of the heated and unheated phases at similar conditions of temperature and LWC shows that a substantial portion of the power increase was attributable to ice accretion on the main rotor blades. These changes in power required represent a significant level flight performance degradation with ice accretion. The full impact of this degradation on the mission profile was not determined.

Table 2. Level Flight Performance.[1]

| Test Temperature (°C) | Average Density Altitude (ft) | Programmed Liquid Water Content (gm/m$^3$) | Immersion Time (min) | Average True Airspeed (kt) | Precloud Engine Shaft Horsepower (hp) | Precloud Gross Weight (lb) | Postcloud Engine Shaft Horsepower (hp) | Postcloud Gross Weight[2] (lb) |
|---|---|---|---|---|---|---|---|---|
| Heated Blade Phase[3] | | | | | | | | |
| -11.5 | 80 | 0.25 | 10 | 88 | 1220 | 15,760 | 1227 | 15,560 |
| -6.5 | 2940 | 0.50 | 22 | 84 | 1146 | 15,720 | 1339 | 15,340 |
| -11.0 | 6680 | 0.25 | 39 | 91 | 1221 | 15,720 | 1317 | 15,080 |
| -6.0 | 6140 | 0.75 | 13 | 92 | 1246 | 15,840 | 1447 | 15,570 |
| -16.5 | -1100 | 0.25 | 48 | 91 | 1258 | 16,080 | 1306[4] | 15,200 |
| -13.0 | 1560 | 0.50 | 29 | 89[5] | 1210 | 15,930 | 1647 | 15,420 |
| Unheated Blade Phase[6] | | | | | | | | |
| -12.5 | -100 | 0.25 | 6 | 91 | 1163 | 16,060 | 1421 | 15,840 |
| -13.5 | -400 | 0.25 | 18 | 90 | 1243 | 16,080 | 1585 | 15,540 |

[1]Rotor speed: 286 rpm (100 percent).
[2]Weight of accreted ice not included.
[3]All deice/anti-ice systems ON.
[4]Cockpit data.
[5]Postcloud airspeed indications unreliable due to fuselage nose ice accretion.
[6]Anti-ice systems ON, deice system OFF.

48. Single-engine topping tests were performed to determine the power-available loss with activation of the anti-ice systems. The tests were conducted at three different temperatures by retarding one engine condition lever (ECL) to START/IDLE and increasing collective pitch control until intermediate rated power was obtained on the operating engine. Data were obtained for each engine with and without the anti-ice systems operating and are presented in figures 1 and 2, appendix G. The average power-available loss with activation of the anti-ice systems was 250 shp per engine for the conditions tested. This represents 16 percent of the power available at -10°C, sea-level conditions. Within the scope of this test, the engine power-available loss due to activation of the anti-ice systems did not limit flight operations.

## AUTOROTATIONAL PERFORMANCE

49. Autorotational descents were performed prior to and following spray cloud immersions to evaluate the effect of airframe and flight control surface ice accretion on autorotational rotor speed and rate of descent. Autorotational descents were conducted at 72 knots calibrated airspeed (KCAS) and maximum attainable rotor speed, but not greater than 300 rpm (105 percent). Autorotational rate of descent, collective control position, and steady-state rotor speed were recorded to evaluate changes in autorotational descent characteristics. A summary of autorotational descent performance is presented in table 3.

50. During the heated blade phase following a 29-minute immersion at test conditions of -13°C and 0.50 gm/m$^3$ LWC, autorotational rate of descent increased from 2500 to 2950 ft/min. During this phase, the increase in rate of descent was not significant and, within the scope of this test, autorotational descent performance is satisfactory.

51. During the unheated blade phase following an 18-minute immersion at -13.5°C and 0.25 gm/m$^3$ LWC, there was a significant increase in autorotational descent rate and a decrease in rotor speed with collective full-down. These changes were attributed to a loss of aerodynamic efficiency of the main rotor blades and a fuselage drag increase caused by ice accretion. Based on the progressive degradation of autorotational performance characteristics observed between the two unheated blade phase flights, it was concluded that increased immersion times would cause further rotor speed degradation, such that minimum safe autorotational rotor speed (90 percent) could not be maintained. The aircraft should be restricted from flight in icing conditions when a deice system is not installed and operating.

## HANDLING QUALITIES

52. The effects of airframe and flight control surface ice accretion on aircraft handling qualities were quantitatively and qualitatively evaluated during both test phases. Quantitative evaluation was accomplished by analysis of level flight control positions measured prior to, during, and following spray cloud immersion.

Table 3. Autorotational Performance.[1]

| Test Phase[2] | Liquid Water Content ($gm/m^3$) | Average Static Outside Air Temperature (°C) | Time in Cloud (min) | Average Density Altitude (ft) | Collective Control Position (% from full-down) | Stabilized Rotor Speed (%) | Rate of Descent (ft/min) | Average Gross Weight (lb) |
|---|---|---|---|---|---|---|---|---|
| A1 | -- | -15.5 | Zero | 3400 | 17.6 | 103 | 2500 | 16,120 |
| A2 | 0.50 | -14.5 | 29 | 880 | 11.9 | 104 | 2950 | 15,300 |
| B1 | -- | -12.0 | Zero | 1280 | 13.6 | 105 | 2600 | 16,100 |
| B2 | 0.25 | -11.0 | 6 | 620 | 11.6 | 104 | 3100 | 15,640 |
| B1 | -- | -11.0 | Zero | 300 | 12.5 | 104 | 2600 | 16,180 |
| B2 | 0.25 | -14.0 | 18 | -371 | Zero | 97.5 | >3500[3] | 15,480 |

[1]Trim airspeed: 72 KCAS.
[2]A1: Heated blade phase, precloud immersion.
A2: Heated blade phase, postcloud immersion.
B1: Unheated blade phase, precloud immersion.
B2: Unheated blade phase, postcloud immersion.
[3]Cockpit data.

Qualitative evaluation was accomplished during and following spray cloud immersion while performing typical instrument flight maneuvers consisting of cruise, 30-degree bank turns, and 500- to 1000-ft/min climbs and descents at 90 knots true airspeed (KTAS). The maximum control position change observed with ice accretion was 4.3 percent (0.3 inch) in the left directional control, which occurred following a 29-minute heated phase immersion at -13°C and 0.50 gm/m$^3$ LWC. This increase in left directional control corresponded to increased power required because of the accreted ice. This change was not noticeable to the pilot. There was no significant change in lateral or longitudinal control position. The only adverse handling quality observed during this evaluation was the aircraft pitch-down discussed in paragraph 39. No other adverse handling qualities attributable to airframe or flight control surface ice accretion and shedding were observed during either test phase.

## VIBRATION CHARACTERISTICS

53. The effects of ice accretion and shedding on aircraft vibration characteristics were evaluated during both test phases. Qualitative evaluation was performed by the test pilots and engineer. Quantitative data were sensed by accelerometers mounted at various places on the airframe (app D) and recorded on magnetic tape. These data were analyzed as described in paragraph 11, appendix E. During the heated blade phase of testing, no qualitative or quantitative changes in vibration characteristics were observed during deice system operation or following spray cloud immersion. During the unheated blade phase, the only change in vibration characteristics occurred following asymmetric shedding of accumulated ice from the main rotor blades. The most pronounced change occurred following 8 minutes of immersion at -13.5°C and 0.25 gm/m$^3$ LWC when a moderate 1-per-rotor-revolution (1/rev) lateral vibration was experienced. This objectionable vibration subsided approximately 1 minute later when additional ice was shed from the main rotor blade.

## HUMAN FACTORS

54. The anti-ice and deice systems control panels were evaluated for location, arrangement, grouping, viewing distance and angles, labeling, and scaling. The pitot heat, engine anti-ice and windshield anti-ice controls were conveniently grouped together and clearly labeled on a single panel located on the overhead switch panel. This panel was conveniently arranged with the cabin heating and windshield wiper controls (photo 8, app H). The deice control panel which contains the generator load meters and blade deice control switches was located above the anti-ice panel on the overhead switch panel. The deice panel was arranged properly, but due to the viewing angle from the pilot seats, the generator load meters could not readily be seen. Observation of the load meter needles is required to monitor deice system operation. The inability to easily view the generator load meters on the overhead switch panel is a shortcoming.

55. The health indicator test (HIT) was a mandatory engine check prior to the first flight of the day. The test consists of setting an engine compressor speed ($N_G$) based on OAT and comparing the indicated $T_{4.5}$ with a base-line temperature. The operator's manual contains base-line temperatures for ambient conditions of -10°C to +50°C. Outside air temperatures less than -10°C were experienced throughout the icing tests. The lack of HIT data in the operator's manual for temperatures less than -10°C precluded the accomplishment of an engine HIT check and is a shortcoming.

56. No cockpit indication of icing severity conditions was provided. The pilot needs to know the icing severity encountered to prevent exceeding the deicing capability of the aircraft. A cockpit icing severity condition indicator should be installed.

## ICE DETECTORS

### General

57. Two special instrumentation ice detectors were installed on the test aircraft to correlate the icing severity levels experienced by the test aircraft with LWC established by the CH-47C spray aircraft. A Rosemount Model 871FA detector was provided by USAAEFA and a Normalair-Garrett detector was provided by the manufacturer. These detectors were not an integral part of the deice system and were evaluated separately. The ice detectors were mounted on an unheated structure located between the pilot door and the right gunner window (fuselage station (FS) 85, right buttline (BL) 46, water line (WL) 150) (photo 3, app D). The detector location and the unheated structure for attaching the detectors to the fuselage were factors which caused inaccurate icing severity indications on both systems at LWC's greater than 0.25 $gm/m^3$.

### Rosemount Ice Detector

58. The Rosemount Model 871FA ice detector provided accurate icing severity information at an LWC of 0.25 $gm/m^3$, but indicated higher than programmed at LWC's of 0.5 and 0.75 $gm/m^3$. At an LWC of 0.25 $gm/m^3$, the detector indicated an icing severity of trace-to-light, which closely correlated with the programmed severity. Indications of moderate-to-heavy icing were observed at an LWC of 0.5 $gm/m^3$ and heavy to full needle deflection at an LWC of 0.75 $gm/m^3$. Except at 0.25 $gm/m^3$ LWC, the detector indicated icing severity higher than programmed. By comparison, data recorded from the Rosemount ice detector mounted on the fuselage nose showed that icing severity indications correlated with the programmed conditions established by the spray aircraft and the visual probe. The test has shown that the Rosemount Model 871FA ice detector will provide accurate icing severity information when properly located on the aircraft.

59. Occasional icing severities of moderate-to-heavy were seen with the aircraft clear of the spray cloud following immersion at LWC's of 0.5 and 0.75 gm/m$^3$. Additionally, moderate icing indications were periodically noted during nonicing flights. The cause of these erroneous indications was not determined.

## Normalair-Garrett Ice Detector

60. The Normalair-Garrett ice detector provided accurate icing severity information at an LWC of 0.25 gm/m$^3$. At LWC's of 0.5 and 0.75 gm/m$^3$, the detector indicated LWC levels higher than programmed. At a programmed LWC of 0.5 gm/m$^3$, the detector indicated 0.5 to 2 gm/m$^3$, with an average of 0.7 gm/m$^3$. At a programmed LWC of 0.75 gm/m$^3$, the detector indicated 1 to 2 gm/m$^3$. These higher than programmed LWC indications follow the same trend observed on the Rosemount detector as discussed in paragraph 57. Moisture shed from the windshield may have contributed to the erroneously high severity indications.

61. The Normalair-Garrett moisture sensing head was housed inside an unheated structure which directed air to the detector probe. Ice accumulations on the detector inlet were observed. The resultant turbulence and restricted airflow possibly interfered with the proper operation of the system. Additionally, erroneous icing severity indications of 0.6 to 1 gm/m$^3$ were observed out of the icing environment after ice had accumulated on the probe housing and the fuselage detector attachment structure. At the selected fuselage location, the Normalair-Garrett ice detector provided accurate indications of icing severity only at an LWC of 0.25 gm/m$^3$.

# CONCLUSIONS

## GENERAL

62. The Boeing Vertol YUH-61A does not possess the capability to safely operate in an icing environment without a rotor deice system.

63. Within the scope of this test, the YUH-61A with an anti-ice/deice system displays excellent potential for operating in a moderate icing environment.

64. The following specific conclusions were reached upon completion of the YUH-61A artificial icing tests:

a. The electrical power requirements of the deice system closely approximated the design estimates (para 15).

b. The engine, engine inlet (D-ring) fairing, engine transmission fairing, windshield, and pitot-static anti-ice systems operated satisfactorily (paras 18, 19, 20, 23, and 26).

c. The cabin heating system operated satisfactorily at OAT's down to -16.5°C (para 28).

d. Damage to the tail rotor blades and tail rotor transmission fairing was observed during the unheated blade phase (para 33).

e. The ship's standard OAT probe operation was satisfactory in an icing environment (para 43).

f. During the unheated blade phase significant power-required increases with ice accretion were noted (para 47).

g. The average power-available loss with activation of the anti-ice systems was 250 shp per engine for the conditions tested (para 48).

h. A significant increase in autorotational descent rate and decrease of rotor speed with collective full-down was noted during the unheated blade phase (para 51).

i. Objectionable lateral vibrations occurred following asymmetric shedding of ice from the main rotor blades during the unheated blade phase (para 53).

j. The Rosemount Model 871FA ice detector provides accurate icing severity information when properly located on the aircraft (para 58).

k. The Rosemount and Normalair-Garrett ice detectors provided accurate ice accretion information only at a test condition of 0.25 $gm/m^3$ LWC (paras 58 and 60).

l. Three deficiencies and nine shortcomings were noted.

## DEFICIENCIES AND SHORTCOMINGS

65. The following deficiencies were identified and are listed in order of importance:

a. Inability to activate the deice system following an ice detector malfunction (para 12).

b. Lack of a system to monitor the IPS turbine operation (para 30).

c. Erratic and unreliable pitot-static indications in level and climbing flight caused by the irregular ice accretion patterns on the lower fuselage nose area (para 40).

66. The following shortcomings were identified and are listed in order of importance:

a. The inability to easily view the generator load meters on the overhead switch panel (para 55).

b. Ice accretion on the cabin heater air inlet on the right forward crown area (para 42).

c. Inaccessibility of the engine transmission oil sight gauge with the heated fairings installed (para 22).

d. Mild switching transients when the deice system is engaged or disengaged (para 14).

e. Lack of ice protection on the center windshield (para 24).

f. Insufficient clearance between the heated engine transmission fairings and the engine transmission oil filler caps (para 21).

g. Lack of HIT data in the operator's manual for temperatures less than -10°C (para 56).

h. Failure of the windshield wipers to return to the PARK position on a dry windshield (para 25).

i. Inadequate heating capacity of the horizontal stabilizer heated surface at test conditions of -13°C and 0.50 $gm/m^3$ LWC (para 35).

# RECOMMENDATIONS

67. Correct the deficiencies prior to flight in icing conditions.

68. Correct the shortcomings prior to production.

69. Conduct testing of the deice/anti-ice systems in natural icing conditions to validate the ice accretion and shedding characteristics and aircraft performance characteristics observed during this evaluation.

70. Conduct an investigation to determine the cause of the illumination of the ROTOR DEICE caution light (para 13).

71. Minimize the exterior protuberances around the pilot and copilot windshields (para 23).

72. Provide ice protection for the pitot tube support strut (para 27).

73. Place the following WARNING in the operator's manual (para 33):

**WARNING**

> Following flight into icing conditions, ice shed from the rotor blades and/or other rotating components presents a hazard to personnel during ground operation and shutdown of the helicopter. Ground personnel should remain well clear of the helicopter during landing, ground operation, and shutdown. Passengers/crewmembers should not exit the helicopter until the rotor has stopped.

74. Redesign the forward crown side work platform supports and upper handholds to reduce ice accretion (para 40).

75. Reduce the fuselage skin protuberances forward of the engine inlets (para 42).

76. Restrict the aircraft from flight in icing conditions when a deicing system is not installed and operating (para 51).

77. Install a cockpit icing severity condition indicator (para 56).

# APPENDIX A. REFERENCES


1. Specification, No. AMC-SS-2222-10000D, UTTAS Project Manager, "System Specification for Utility Tactical Transport Aircraft System," 10 November 1975.

2. Letter, AVSCOM, DRSAV-EQI, 25 May 1976, subject: Utility Tactical Transport Aircraft System (UTTAS), Artificial Icing Test, AVSCOM Test Request, Project No. 76-09.

3. Test Plan, USAAEFA, Project No. 76-09, *Artificial Icing Tests, Utility Tactical Transport Aircraft System (UTTAS), Sikorsky YUH-60A Helicopter, Boeing YUH-61A Helicopter*, August 1976.

4. Prime Item Development Specification, AMC-CP-222-V1000A, Boeing Vertol Company, "UTTAS," Revision 4, March 1976.

5. Technical Manual, Boeing Vertol Company, Contract No. DAA501-73-C-0007, *Operator's Manual, Utility Tactical Transport Aircraft System, YUH-61A*, 1 March 1976, revised 1 July 1976, with Icing Supplement, 27 September 1976.

6. Final Report, USAAEFA, Project No. 74-06-2, *Goverment Competitive Test, Utility Tactical Transport Aircraft System (UTTAS), Boeing YUH-61A Helicopter*, to be published.

7. Technical Manual, All American Engineering Company, SM 280B, *Installation, Operation, and Maintenance Instructions With List of Parts, Helicopter Icing Spray System (HISS)*, 12 November 1973, with Change 1, 15 July 1976.

8. Technical Report, Environmental Research and Technology Inc, *Characteristics of a Spray Plume*, April 1976.

9. Letter, AVSCOM, DRSAV-EQI, 27 September 1976, subject: Safety-of-Flight Release for the YUH-61A Artificial Icing Test.

10. Message, AVSCOM, DRSAV-EQI, 301525Z September 1976, subject: Revised Safety-of-Flight Release for the YUH-61A Artificial Icing Test.

11. Instruction Manual, Rosemount Engineering Company, No. 8748, *Ice Detector Model 871FA*, August 1974.

12. Technical Proposal, Normalair-Garrett Ltd, No. 1029, Issue 5, *Ice Detector System (Inferential Type)*, January 1975.

13. Technical Report, Calspan Inc, No. CG-5391-M-1, *Measurement of the Microphysical Properties of a Water Cloud Generated by an Airborne Spray System*, December 1973.

14. Final Report, USAAEFA, Project No. 75-04, *Modified Helicopter Icing Spray System Evaluation*, to be published.

15. Field Manual, FM 1-30, *Meteorology for Army Aviators*, 31 May 1976.

16. Army Regulation, AR 310-25, *Dictionary of United States Army Terms (short title: AD)*, 1 March 1969.

# APPENDIX B.

# DEICE/ANTI-ICE SYSTEMS DESCRIPTION

## GENERAL

1. The YUH-61A deice system provides the capability to deice the main rotor blades, tail rotor blades, and the horizontal stabilizer. The location of the major components on the aircraft is shown in figure 1. A detailed listing of all the system components is shown below. Total weight of the components, except the main and tail rotor deice blankets, is 82.5 pounds. The aircraft also incorporates systems which provide anti-ice capability for integral components of the engines, engine inlet and transmission, pilot and copilot windshields, and pitot tubes. The deice/anti-ice systems are described in this appendix.

### Control System

Deicing controller
Control panel
Ice detector
Air temperature sensor
Power contactors
Current transformers

### Main Rotor

Deice blankets (4)
Rotor blade cable assemblies (4)
Rotor shaft cable assembly
Distributor assembly
Slip ring and adaptor

### Tail Rotor

Deice blankets (4)
Rotor blade cable assemblies (4)
Rotor shaft cable assembly
Slip ring
Terminal board

### Horizontal Stabilizer

Deice blankets (2)
Temperature controllers (2)
Relays and sockets (2)

### Miscellaneous

Cable assemblies
Circuit breakers

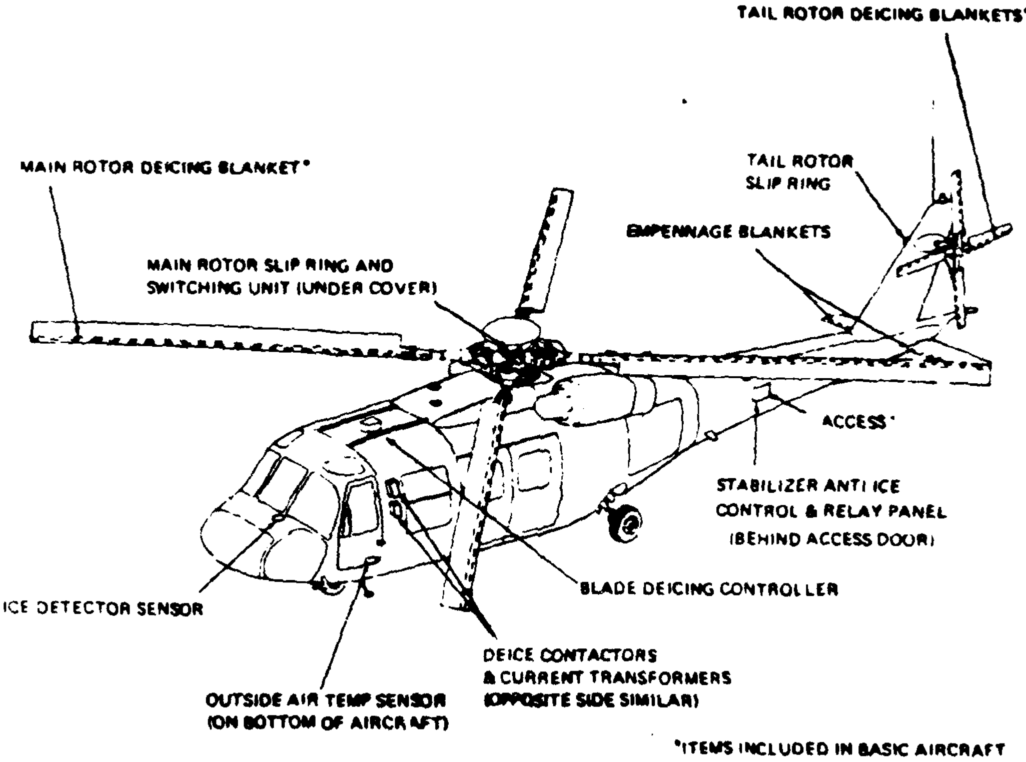


Figure 1. Deice System Major Components.

## DEICE SYSTEM

### Main Rotor Blades

2. The main rotor blades are fabricated with electrothermal deicing blankets installed as part of the blade leading edge assembly (fig. 2). The heater elements provide a power density of 28 watts per square inch. The heating elements cover the forward 11 percent of the chord on the upper surface at the inboard end, increasing to approximately 12 percent at the blade tip. On the lower surface, the heating elements cover the forward 24 percent of the chord at the inboard end and increase to 25 percent at the blade tip. The heating elements consist of 10 blankets on each blade, 5 major (11 ohms) and 5 minor (5.5 ohms) (fig. 3). A maximum 3-phase electrical load of 21.8 kilowatts is required to deice the main rotor blades.

### Tail Rotor Blades

3. Each tail rotor blade (fig. 4) is protected by a single-element deicing blanket. The blanket covers approximately 10 percent of the chord on both sides of the blade along the leading edge. The heating elements provide a power density of 28 watts per square inch. The total tail rotor load of 8.8 kilowatts is carried by two of the three power phases.

### Horizontal Stabilizer

4. An electrothermal deicing blanket is bonded to the leading edge of each horizontal stabilizer (fig. 5). Each blanket consists of a 1-inch-wide anti-iced parting strip along the leading edge and a 3-inch-wide cyclically heated deice element on both sides of the leading edge. When the deice system is operating, a continuous temperature of approximately 150°F is maintained on the parting strip by a temperature sensor and temperature controller. The electrical power requirement for the two parting strips is 2.15 kilowatts. The deice elements provide a power density of 20 watts per square inch and require a total electrical load of 14.5 kilowatts.

### Control System

5. The control system consists of a cockpit control panel, a deice controller, an OAT sensor, an ice detector, slip rings, and cabling. Additionally, current transformers are used to monitor system loads. The cockpit control panel (fig. 6) contains an ON/OFF switch, an override switch, a test button, and a dual-needle load meter. Their functions are discussed in paragraphs 7 through 11. The deice controller contains the necessary electronics and main power switching contactors to activate the deicing subsystems. The switching contactors sequence the electrical power to the main rotor blade, tail rotor blade, and horizontal stabilizer deicing blankets. The deice controller is mounted in the cabin roof, as shown in figure 1. The OAT sensor is located beneath the fuselage and provides temperature information to the deice controller. A Rosemount Model 871FA ice detector is

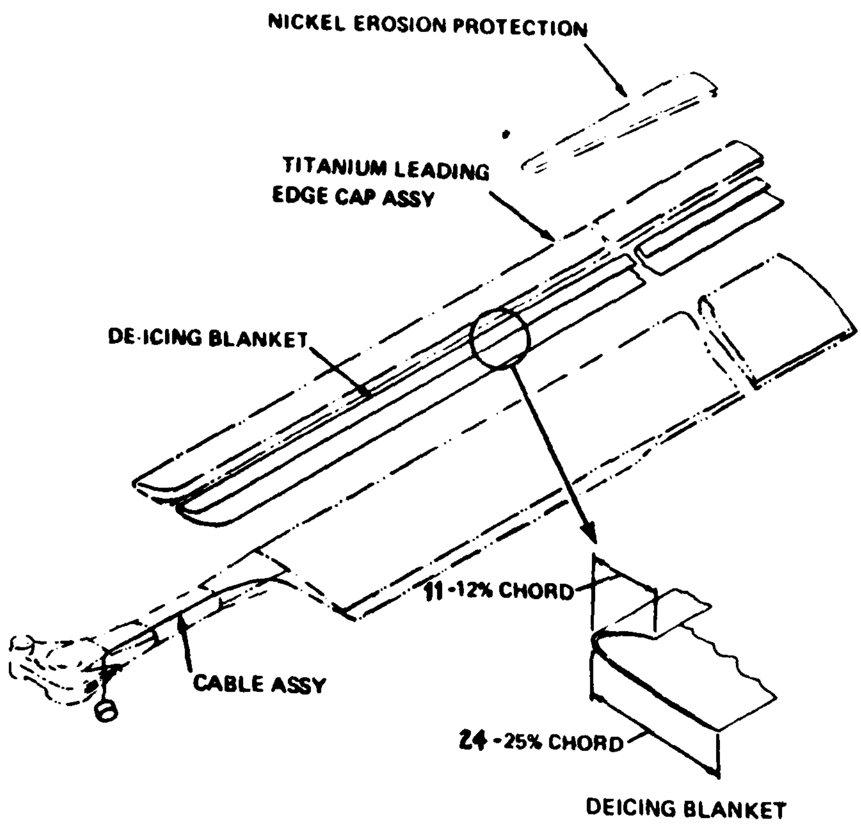


Figure 2. Main Rotor Blade Deicing Blanket Location.

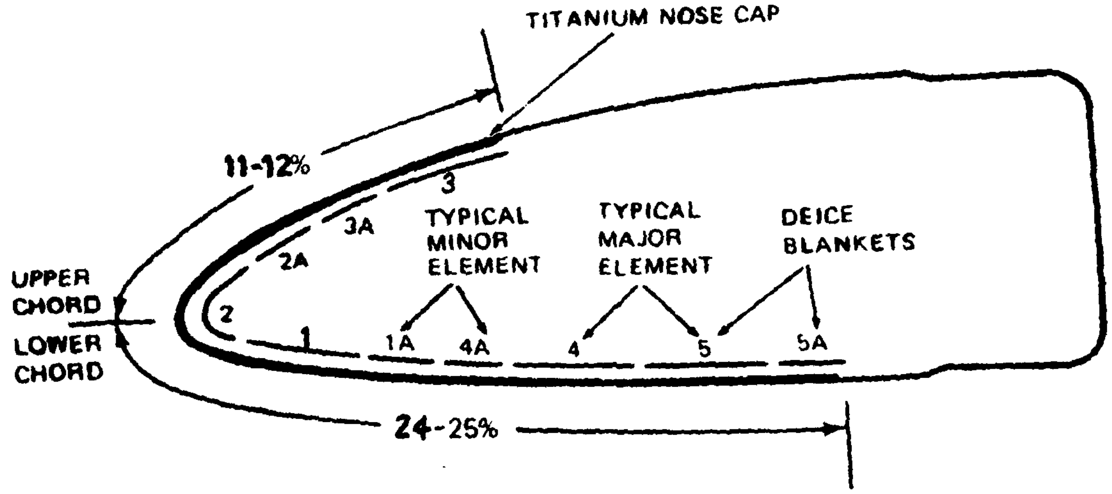


Figure 3. Main Rotor Blade Deicing Blanket Arrangement.

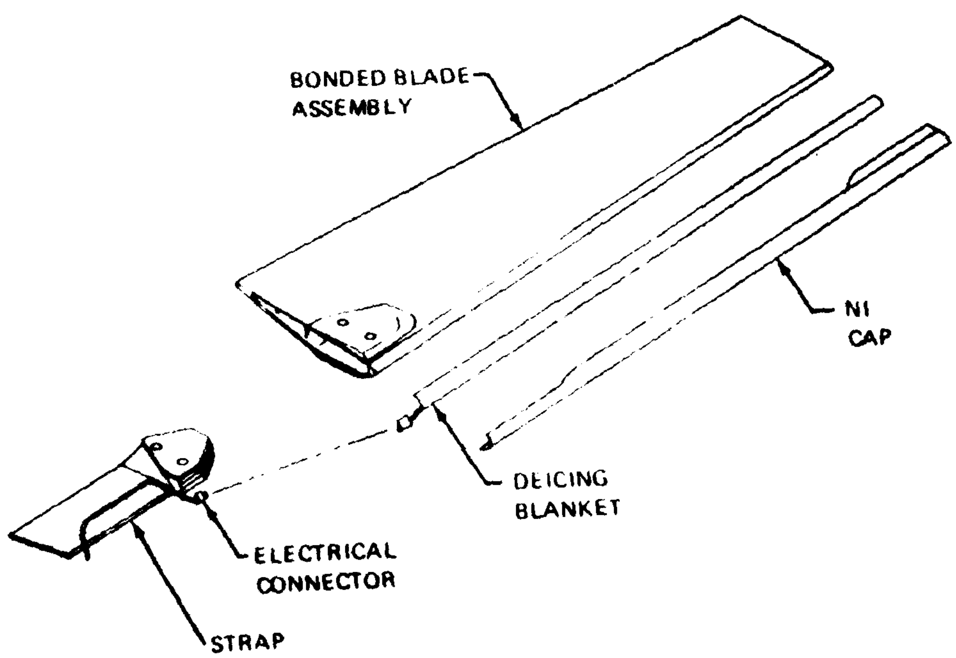


Figure 4. Tail Rotor Blade Deicing Blanket Location.

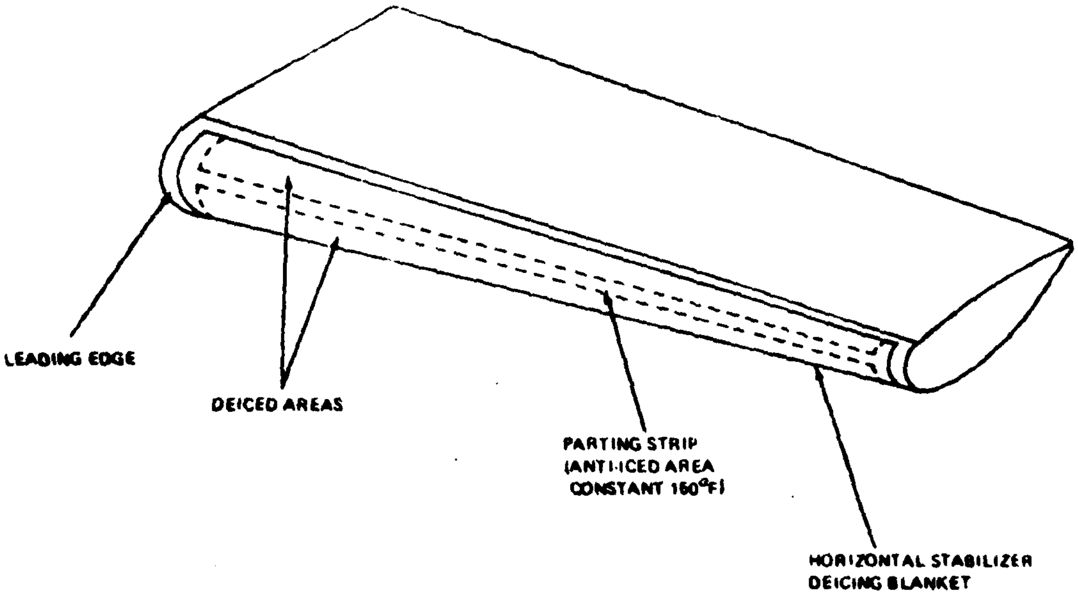


Figure 5. Horizontal Stabilizer Deicing Blanket Location.

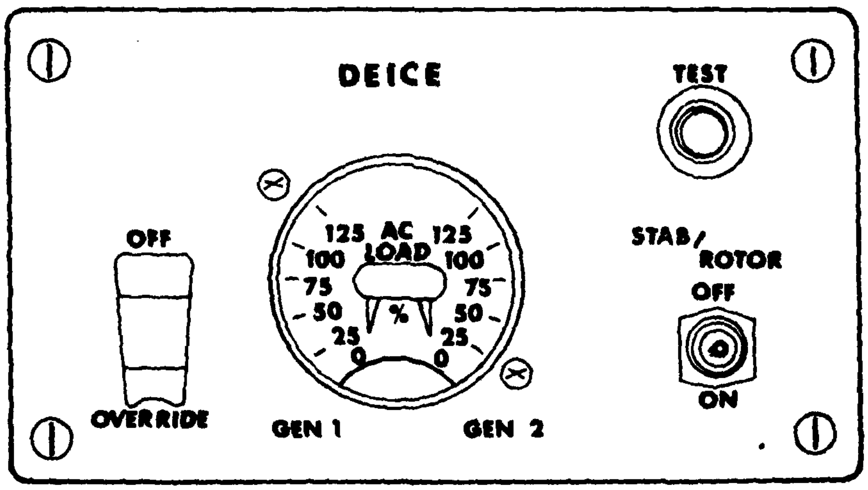


Figure 6. Cockpit Control Panel.

located on the aircraft nose forward of the copilot windshield and provides ice accretion information to the deice controller (photo 1). A description of the ice detector is contained in appendix D. Electrical power reaches the main and tail rotor blankets through slip ring and distributor assemblies.

Photo 1. Deice System Rosemount Ice Detector.

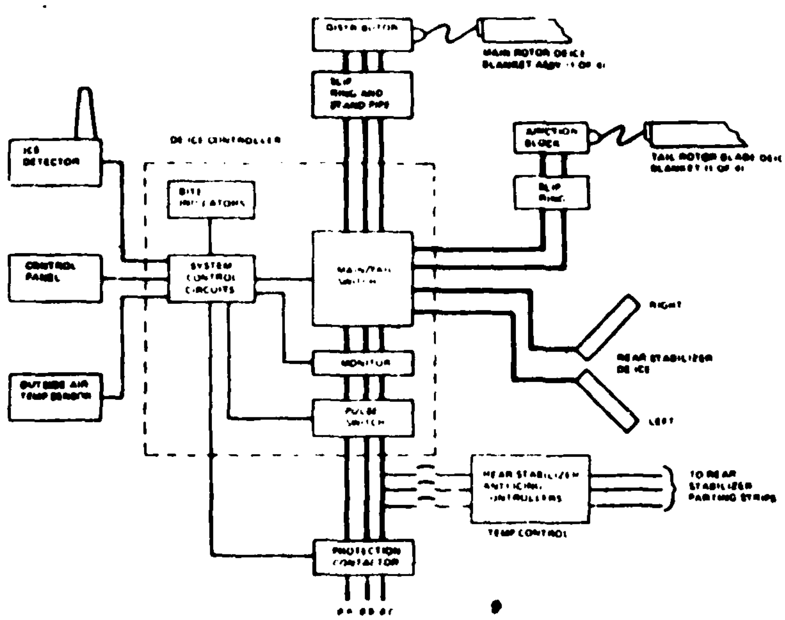

Figure 7. Deicing System Schematic.

## System Operation

6. A system schematic is shown in figure 7. The sequence of a typical deice cycle is shown in figure 8. Generally, the system allows ice accretion and then deices, based on OAT and ice accretion rate.

7. The ROTOR/STAB switch on the cockpit control panel is placed ON to energize the deice system. This switches all the normal aircraft electrical loads to the No. 1 generator and energizes the ice detector and the horizontal stabilizer parting strips. All the electrical power necessary to operate the deice system is supplied by the No. 2 generator.

8. In the event of failure of the No. 2 generator, the OVERRIDE switch is placed in the ON position and the No. 1 generator is used to furnish the required electrical power for deice system operation. If this occurs, nonessential electrical requirements may be curtailed to remain within single generator output capacity. The ice detector senses the presence of ice by monitoring the natural frequency of a magnetostrictive element. The deice system ice detector is similar in operation to the special Rosemount instrumentation discussed in paragraph 11, appendix D. Basically, as ice is accreted on the detectors, the natural frequency lowers. When the frequency is lower than a preset limit (0.020 inch of ice), a discrete signal is sent to the deice controller unit. The accreted ice is then heat purged from the detector and the controller stores an ice count of 1. Ice is again allowed to accrete on the detector until a second ice pulse occurs. Upon receipt of the second pulse, the controller unit sends a power pulse to the four tail rotor blade heating

blankets. While power is being applied to the tail rotor blankets, the ice detector is again purged and the ice count remains on 2. Ice is accreted again for two more counts. Upon receipt of the fourth count, the controller unit initiates a full deice cycle.

9. A full cycle consists of 12 power pulses. As shown in figure 8, the first power pulse goes to the tail rotor; the next five pulses to main rotor blades No. 1 and No. 3 simultaneously; the next five pulses to main rotor blades No. 2 and No. 4 simultaneously; and the last pulse to the horizontal stabilizer. The main rotor blade deicing elements are energized sequentially from the leading edge toward the trailing edge. Major and minor blankets on opposing blades are energized simultaneously to promote symmetrical shedding. All four tail rotor blades are energized simultaneously. The pulse duration time is dependent on OAT and varies from 0.15 second at 0°C to 26 seconds at -25°C.

10. Ice counts which occur during a deicing cycle are retained by the controller. A complete deicing cycle or a tail rotor deicing cycle will be automatically initiated following a previous cycle, depending on the number of ice counts received by the deice controller.

11. The system can be tested using the test button on the cockpit control panel. With the ROTOR/STAB switch ON and both generators operating, the test button is depressed twice. The controller then sends a power pulse to the tail rotor blades. To initiate the entire deicing sequence, the test button is depressed twice more. The controller now sends power to the tail rotor blades, main rotor blades, and the horizontal stabilizer. Each power pulse is indicated on the dual-needle load meter as a momentary needle fluctuation.

Fault Detection

12. The deice system incorporates fault detection circuitry within the deice controller. Detectable faults are listed below. The occurrence of any one of the listed faults will stop the deice sequence, trip a built-in test element (BITE) indicator on the deice controller box, and activate the master caution light and ROTOR DEICE caution light on the instrument panel. Detection of the listed faults is accomplished by a combination of 3-phase voltage and current measurements and time measurements.

Undervoltage
Failure to advance switch unit
Counter failure
OAT sensor failure
No current
Overcurrent
Current unbalance
Main rotor fault
Stabilizer fault
Ground current fault

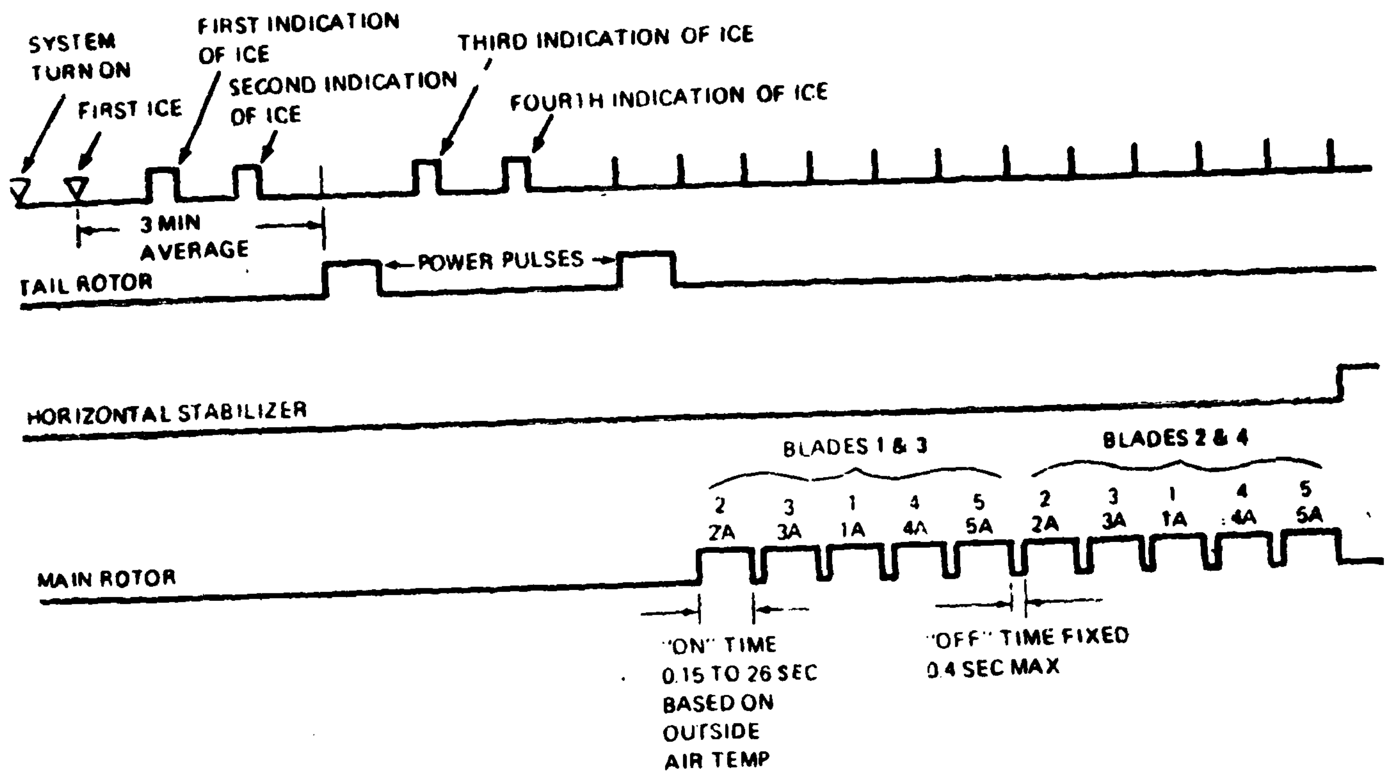


Figure 8. Deice Sequence.

blankets. While power is being applied to the tail rotor blankets, the ice detector is again purged and the ice count remains on 2. Ice is accreted again for two more counts. Upon receipt of the fourth count, the controller unit initiates a full deice cycle.

9. A full cycle consists of 12 power pulses. As shown in figure 8, the first power pulse goes to the tail rotor; the next five pulses to main rotor blades No. 1 and No. 3 simultaneously; the next five pulses to main rotor blades No. 2 and No. 4 simultaneously; and the last pulse to the horizontal stabilizer. The main rotor blade deicing elements are energized sequentially from the leading edge toward the trailing edge. Major and minor blankets on opposing blades are energized simultaneously to promote symmetrical shedding. All four tail rotor blades are energized simultaneously. The pulse duration time is dependent on OAT and varies from 0.15 second at 0°C to 26 seconds at -25°C.

10. Ice counts which occur during a deicing cycle are retained by the controller. A complete deicing cycle or a tail rotor deicing cycle will be automatically initiated following a previous cycle, depending on the number of ice counts received by the deice controller.

11. The system can be tested using the test button on the cockpit control panel. With the ROTOR/STAB switch ON and both generators operating, the test button is depressed twice. The controller then sends a power pulse to the tail rotor blades. To initiate the entire deicing sequence, the test button is depressed twice more. The controller now sends power to the tail rotor blades, main rotor blades, and the horizontal stabilizer. Each power pulse is indicated on the dual-needle load meter as a momentary needle fluctuation.

**Fault Detection**

12. The deice system incorporates fault detection circuitry within the deice controller. Detectable faults are listed below. The occurrence of any one of the listed faults will stop the deice sequence, trip a built-in test element (BITE) indicator on the deice controller box, and activate the master caution light and ROTOR DEICE caution light on the instrument panel. Detection of the listed faults is accomplished by a combination of 3-phase voltage and current measurements and time measurements.

Undervoltage
Failure to advance switch unit
Counter failure
OAT sensor failure
No current
Overcurrent
Current unbalance
Main rotor fault
Stabilizer fault
Ground current fault

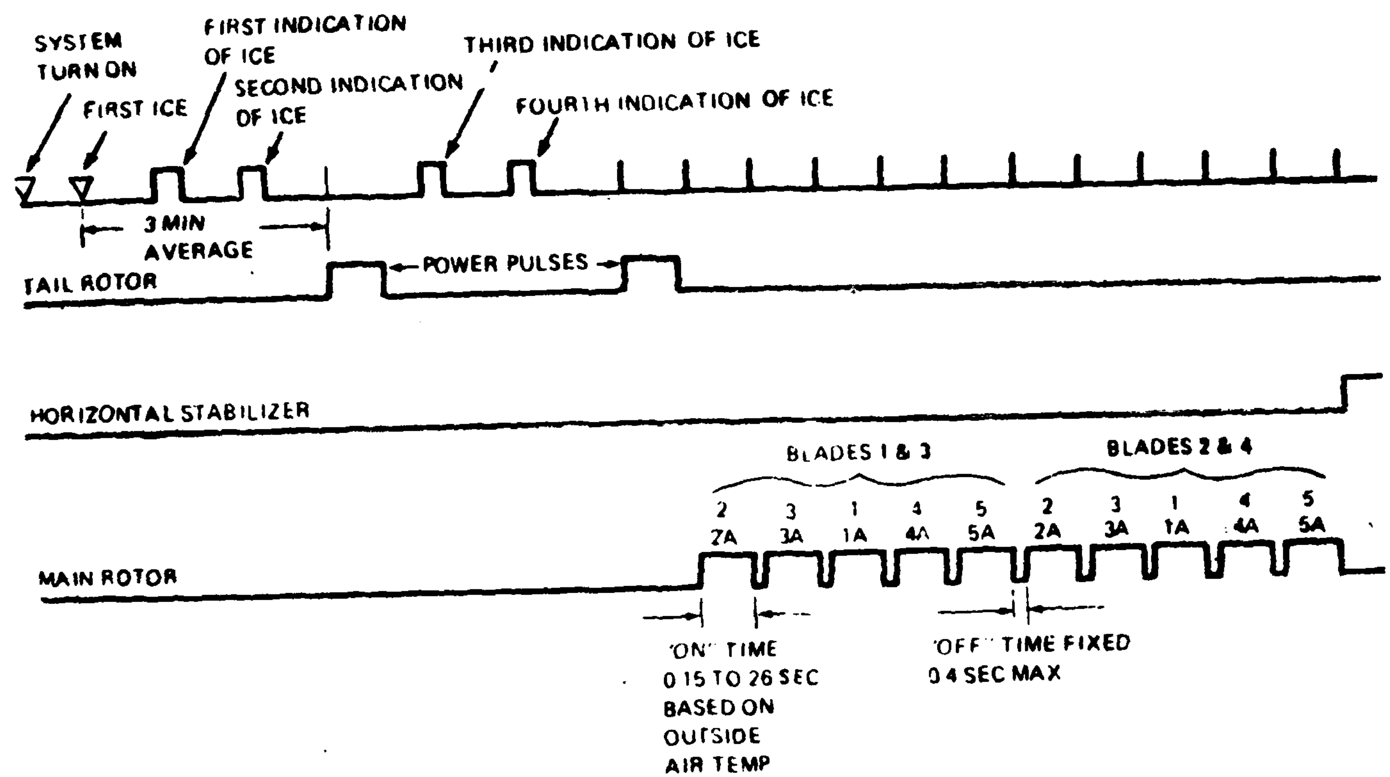


Figure 8. Deice Sequence.

Excessive heat ON time
Excessive heat OFF time
Deice controller failure
Switch unit failure

## ANTI-ICE SYSTEMS

### Engine Anti-Icing

13. Engine anti-icing is accomplished by a combination of hot axial compressor discharge air and heat transfer from the air/oil cooler which is integral to the main engine frame. A hot-air anti-icing valve is electrically controlled by the ENG INLET switch on the overhead panel. Anti-icing is OFF when electrical power is applied to the solenoid of the combination anti-icing and starting bleed valve assembly (*ie*, the system fails ON). Additionally, the valve will automatically open and provide anti-icing air at an $N_G$ less than 83 percent.

14. Axial compressor discharge air (stage 5) is bled from the compressor casing at the 7 o'clock position, routed through the anti-icing valve, and delivered to the front frame and swirl frame via ducting (fig. 9). Within the swirl frame, hot air is ducted around the outer casing to each swirl vane. The hot air is circulated within each vane by a series of baffles and then exits from two areas into the engine inlet. Approximately 90 percent of this hot air exits at the vane outer trailing edges. The other 10 percent exits through a series of circumferential slots in the swirl frame hub at the aft edge, which acts to preclude water from adhering to the hub and flowing into the compressor. Front frame anti-icing air flows through a cored passage in the main frame to the front frame nose splitter, then exits to the main frame scroll and is discharged into the IPS air flow.

15. Anti-icing air is also ducted to the compressor inlet guide vanes (IGV's). A circumferential manifold surrounds the aft flange of the main frame to distribute hot air to the hollow IGV's. Slots in the trailing edges of the IGV's discharge this flow into the compressor inlet. Additionally, hot scavenge oil passing within the scroll vanes in the main frame precludes ice build-up which could result from moisture-laden IPS air.

### Engine Air Induction Anti-icing

**Engine Inlet (D-Ring) Fairing:**

16. The engine inlet fairing is anti-iced by hot bleed air from the engine compressor. The bleed air is directed from the compressor discharge port through the engine inlet anti-ice valve to the fairing. As shown in figure 9, the fairing contains a circular duct which circulates the bleed air to numerous bleed ports on the inner and outer circumference. Operation of the engine inlet anti-ice valve is controlled by the ENG INLET switch on the overhead panel.

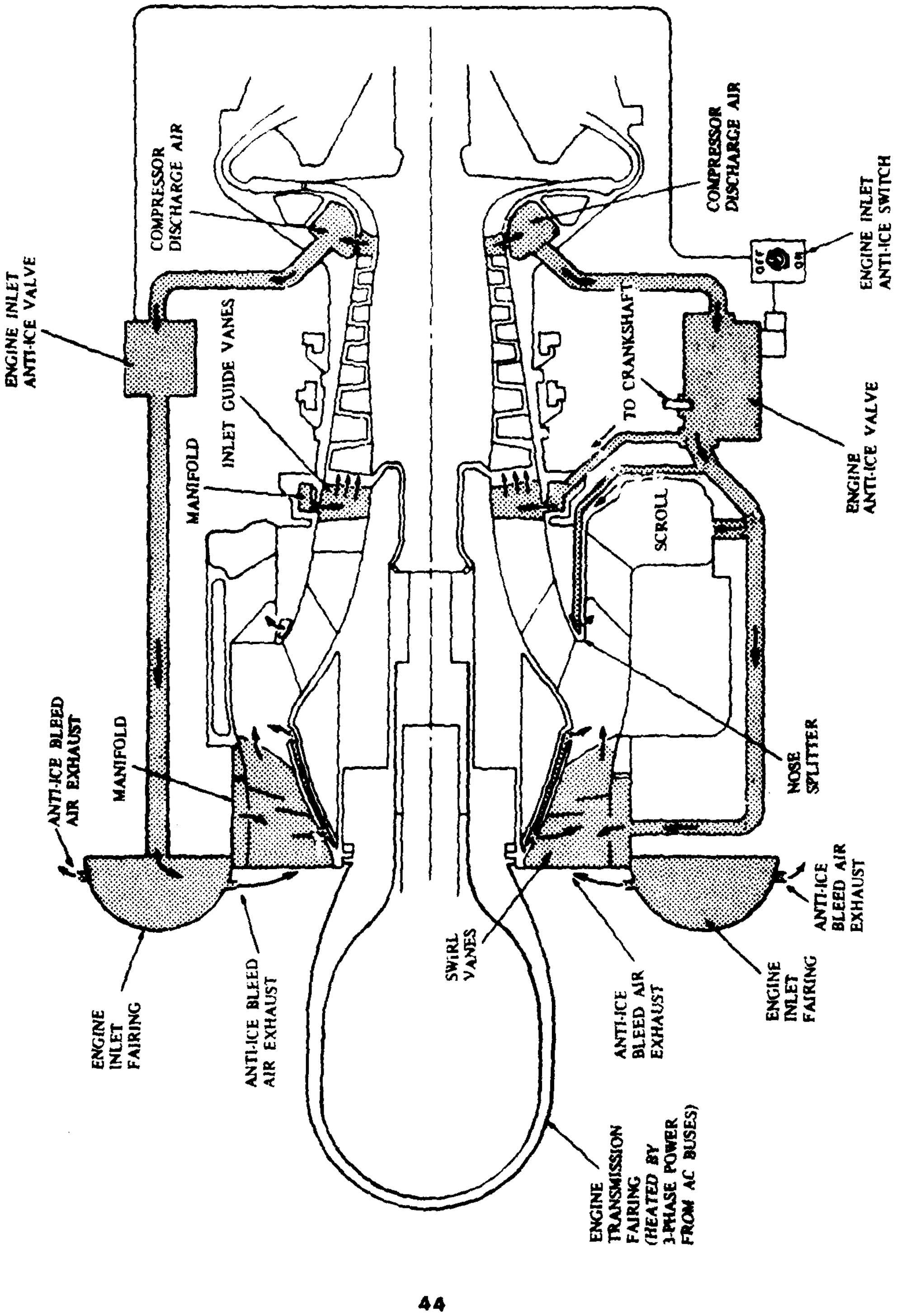


Figure 9. Engine and Engine Air Induction Anti-Icing Schematic.

**Engine Transmission Fairing:**

17. The engine transmission fairing and cross-shaft fairing are anti-iced by electric heating elements embedded in the fairings (fig. 9). Electrical power to the heating elements is from the 3-phase AC buses through 3-ampere ANTI-ICE ENG circuit breakers on the AC distribution panels. A temperature sensor embedded in each fairing disconnects electrical power to the fairing when the fairing temperature rises above 35°C (95°F). Operation of the electric heating elements is controlled by the ENG INLET switch on the overhead panel.

**Engine Inlet Anti-Ice Switch and Advisory Lights**

18. The two-position ENG INLET anti-ice switch is located on the overhead panel. When this switch is placed ON, the engine inlet anti-ice valve and the engine anti-ice valve (fig. 9) are opened. Compressor discharge air will then flow through both the engine anti-ice system (paras 14 and 15) and the engine inlet fairing (para 16). The engine anti-ice relay also closes, and 3-phase AC power heats the engine transmission fairing (para 17). Two green engine anti-ice advisory lights are located on the annunciator panel. When illuminated, these lights indicate that the ENG INLET anti-ice switch is ON, the engine and engine inlet anti-ice valves are open, and the engine transmission fairing temperature is above 4 to 6°C (39 to 43°F).

**Windshield Anti-Ice System**

19. The pilot and copilot windshields have independent electrothermal anti-icing systems. Each windshield has a thin film heating element embedded between the inner acrylic and outer glass layers. A temperature sensor is also embedded in each windshield. Electrical power to the windshield anti-ice system is controlled by the PILOT and COPILOT WSHLD switches on the overhead panel. When the switches are placed ON, a controller in the overhead panel applies electrical power intermittently to the windshield heating elements to maintain a temperature between 40.5 to 44.5°C (105 to 112°F).

**Pitot Tube Anti-Ice**

20. Each pitot tube has an integral heating element. Electrical power is applied to the heaters through the PITOT HTR switch on the overhead panel.

# APPENDIX C. HELICOPTER ICING SPRAY SYSTEM DESCRIPTION

1. The HISS is carried on board a CH-47C aircraft. The icing spray system equipment consists of a spray boom, boom supports, boom hydraulic actuators, an 1800-gallon unpressurized water tank, and operator control equipment (fig. 1). The spray boom consists of two 27-foot center sections and two 16.5-foot outer sections. The total weight of the system is approximately 4700 pounds empty. With the boom fully extended, the upper center section is located in a horizontal plane 15 feet below the aircraft and the lower center section 20 feet below. The booms are fully jettisonable in both the fully extended and stowed positions. The water is also jettisonable (total load of 1800 gallons) in approximately 10 seconds with the boom in any position. A total of 174 nozzle locations are provided on the spray boom. Nozzles are installed at 54 of these locations. A bleed air supply from the aircraft engines is used to atomize the water at the nozzles. For a more detailed description of the icing spray system, see reference 7, appendix A.

2. The LWC and water droplet size distribution of the spray cloud are controlled by varying the water flow rate and the distance of the test aircraft behind the spray aircraft. Controls and indicators for the water flow rate and bleed air pressure are located on the water supply tank. A radar altimeter is mounted in the rear cargo door opening of the CH-47C and is directed aft. The distance between the test and spray aircraft is measured by the radar altimeter and the information is presented in the spray aircraft cockpit. The methods used to establish the desired LWC are presented in appendix E. A detailed description of the spray cloud characteristics is contained in reference 8, appendix A.

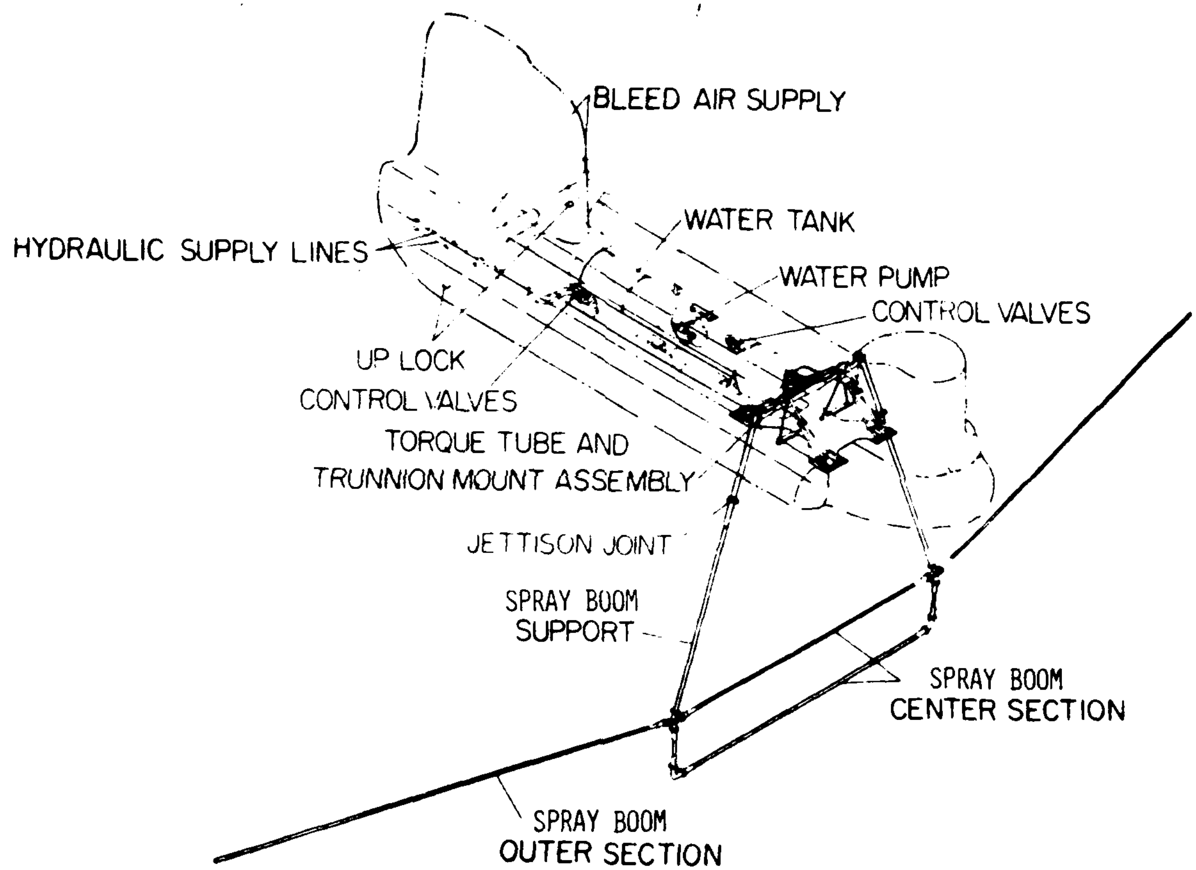


Figure 1. HISS Schematic.

# APPENDIX D.

# INSTRUMENTATION AND SPECIAL EQUIPMENT

## INSTRUMENTATION

1. In addition to, or instead of, standard aircraft instruments, sensitive calibrated instrumentation was installed aboard the test aircraft and maintained by the contractor. Data were recorded from the cockpit instrumentation and specially installed instrumentation system. Data were recorded on flight data cards and magnetic tape (PCM and FM). Selected parameters were observed real time via air-to-ground telemetry. Flight crew comments were recorded on a portable tape recorder.

2. The sensitive instrumentation, calibrated ship's system instrumentation, and related special equipment installed are listed below.

### Pilot Station

Data recorder switch
Event switch

### Pilot Panel

Airspeed
Altitude (ship's system)
Altitude (radar)
Rotor speed (digital)
Rotor speed (ship's system)
Engine torque (both engines)
Engine turbine gas temperature (both engines)
Engine gas generator speed (both engines)
Control position:
- Longitudinal
- Lateral
- Directional
- Collective
- Tail rotor slider

Horizontal tail position
Center-of-gravity normal acceleration

### Copilot/Engineer Station

Instrumentation controls and lights
On-board camera controls and lights
Data recorder switch
Event switch
Visual ice accretion probe

**Copilot/Engineer Panel**

Airspeed
Altitude
Rotor speed
Engine torque (both engines)
Free air temperature
Main rotor blade temperature
Fuel used (both engines)
Deice system ice detector signal light
Rosemount icing rate
Normalair-Garrett icing condition
Integral particle separator duct differential
    pressure (both engines)
Time code display
Run number

**Digital (PCM) Data Parameters**

Airspeed
Altitude (ship's system)
Altitude (radar)
Rate of climb
Free air temperature
Rotor speed
Engine gas generator speed (both engines)
Engine power turbine speed (both engines)
Engine output shaft torque (both engines)
Engine turbine gas temperature (both engines)
Fuel flow (both engines)
Fuel used (both engines)
Integral particle separator duct differential
    pressure (both engines)
Control position:
    Longitudinal
    Lateral
    Directional
    Collective
    Engine condition lever (both engines)
Tail rotor slider
Yaw compensator actuator position
Horizontal tail position
Main rotor shaft bending

Main rotor and tail rotor cameras:
- Correlation pulse
- Run command
- Failure signal
- Out of phase signal
- Film used

Engine transmission nose fairing temperature (both engines)
Engine transmission fairing fold temperature (both engines)
Main rotor blade blanket temperature
Generator No. 1:
- Frequency
- Voltage (A, B, and C phase)
- Current (A, B, and C phase)

Deice/anti-ice systems electrical parameters:
- Main rotor voltage (A phase)
- Main rotor current (A phase)
- Tail rotor voltage (A-B and B-C phase)
- Tail rotor current (A and C phase)
- Horizontal stabilizer voltage (left and right side)
- Horizontal stabilizer current (left and right side)
- Engine transmission fairing voltage (No. 1 engine)
- Engine transmission fairing current (No. 1 engine)
- Windshield voltage (single-phase)
- Windshield current (single-phase)

Rosemount icing rate (instrumentation system)
Rosemount icing rate (ship's system)
Normalair-Garrett icing condition
Pitch attitude
Roll attitude
Time code
Run number
Event marker

**Analog (FM) Data Parameters**

Main rotor blade camera correlation
Event marker
Voice

Vibration (accelerometers):
- Pilot seat (vertical, lateral, and longitudinal)
- Copilot seat (vertical, lateral, and longitudinal)
- Instrument panel (right side vertical and lateral)
- Instrument panel (left side vertical)
- Center of gravity (vertical, lateral, and longitudinal)
- Main rotor transmission (vertical, lateral, and longitudinal)
- Tail rotor transmission (vertical, lateral, and longitudinal)

3. In addition to standard aircraft instruments, sensitive calibrated instrumentation was installed aboard the CH-47C spray aircraft. This instrumentation was used to establish the desired test conditions during the icing flights and is listed below.

- Airspeed
- Altitude
- Free air temperature
- Dew point
- Water flow rate
- Bleed air pressure
- Radar distance (separation between test and spray aircraft)

## SPECIAL EQUIPMENT

### Camera Systems

4. Two 16mm high-speed, hand-held motion picture cameras were used to document ice accretion characteristics of the test aircraft. One camera was located on board the CH-47C spray aircraft and was used while the test aircraft was in the spray cloud. The other camera was located on board the chase aircraft and was used to document the test aircraft both in the spray cloud and after exit from the cloud. Additionally, 35mm slide and black and white still cameras were used for documentation both in the air and on the ground following each icing flight.

5. In addition to the chase and HISS high-speed photography, documentation of main and tail rotor condition was achieved using nonrotating 16mm high-speed cameras mounted on board the test aircraft. The main rotor blade camera was located in the cargo compartment and viewed the lower surface of the main rotor blades through the right-hand forward cargo door window (photo 1). A second camera, mounted on the left side of the tail boom at the fold hinge, was used to photograph the leading edge of the tail rotor blades and a section of the left-hand horizontal stabilizer (photo 2). A camera control panel was mounted just aft of the cockpit center console with one master power switch and a run switch (ON-OFF) for each camera. With the master power switch ON, power was supplied to the camera motors, electronics, and heaters.

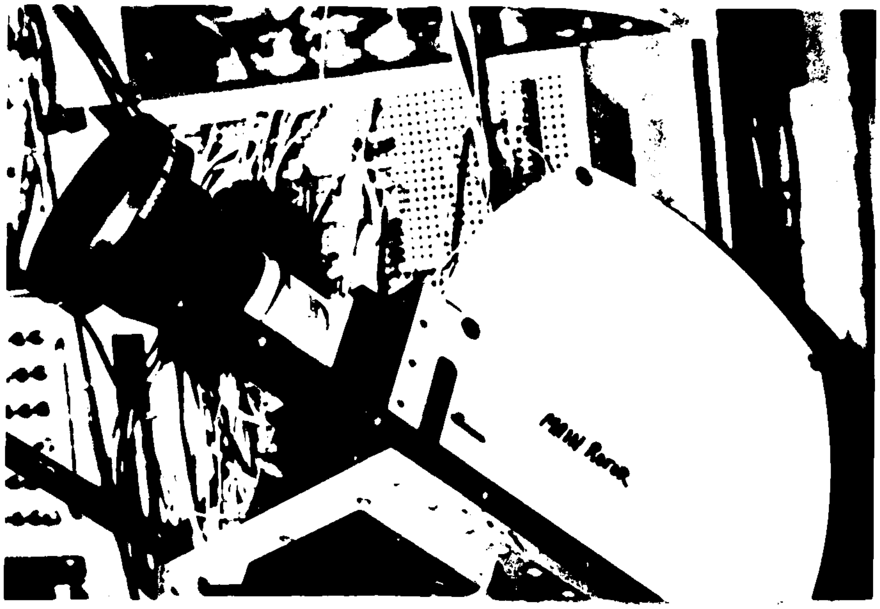

Photo 1. Main Rotor Camera Installation.

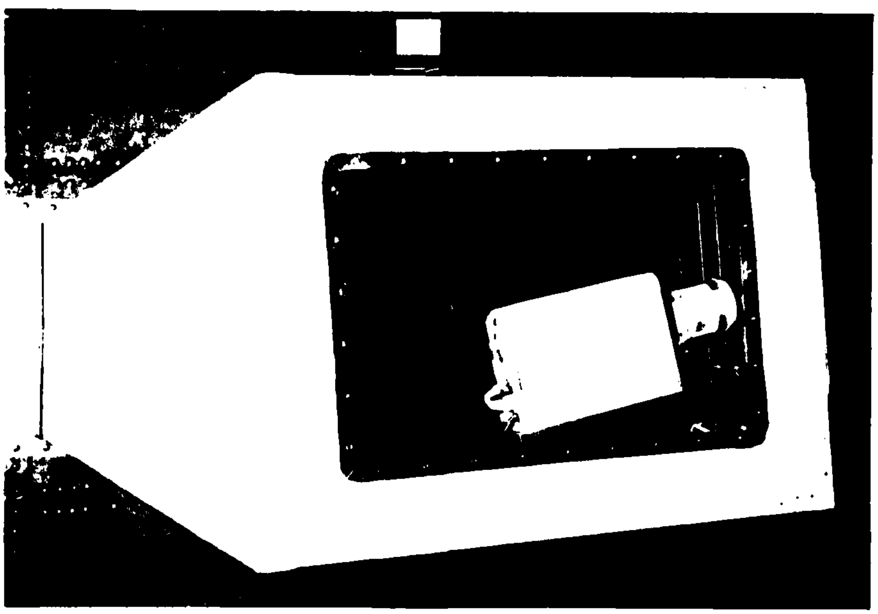

Photo 2. Tail Rotor Camera Installation.

6. The cameras, manufactured by Photo-Sonic Inc, were 16mm Model IPL cameras with phase lock kits and 1200-foot film magazines. Shutter speeds of 16 to 500 frames per second could be selected. The cameras were synchronized to photograph the blades at fixed aircraft azimuths. Synchronization was achieved by triggering the camera shutter through the phase lock kit with a multiplexed and phase compensated 1/rev signal. The main rotor camera had the capability of photographing blades at four or eight frames per rotor revolution. Shutter speeds up to 1/1800 second were used at four frames per revolution. The tail rotor camera had the capability for synchronization at one or two frames per tail rotor revolution. Design characteristics are listed below.

| | |
|---|---|
| Temperature | -65 to +160°F |
| Vibration | 5 to 17 Hz at 0.7-inch double amplitude |
| | 17 to 4000 Hz at 10g |
| Acceleration | 25g (three major axes) |

7. The main rotor blade camera was mounted on a square cross-section beam attached to the vertical aircraft support structure at FS 129 and 201 on the right side of the cabin interior. The span of the beam was the span of the cargo door opening. A Winter Engineering Company Model 1610B mount with two degrees of adjustment (pitch and yaw) and quick-disconnect features was attached to the beam for camera mounting. A 5.3mm lens was used on the main rotor camera, which provided a field of view from inboard of the pendulum vibration absorbers to the blade tips.

8. The tail rotor camera was mounted in a water-tight box attached to the left-hand side of the tail boom at the tail fold hinges. A secondary support attachment was made at the first vertical aircraft support forward of the fold hinge. The camera was mounted inside the box on a Winter Engineering Company mount. A heated window provided by Pittsburg Plate Glass was used to ensure a clear viewing surface.

## Icing Detectors

**General:**

9. Two icing detectors were installed on the test aircraft to correlate the icing severity levels experienced by the test aircraft with the LWC established by the CH-47C spray aircraft. A third ice detector was installed as an integral component of the aircraft deice system (para 5, app B). A visual ice accretion probe was also installed on the test aircraft to observe icing rates. These items are described in the following paragraphs.

**Rosemount Ice Detector:**

10. The Rosemount Model 871FA ice detector is an electromechanical device which transmits an electronic signal when a specified thickness of ice is present on the sensing probe. Two Model 871FA detectors were mounted on the test aircraft. The Boeing Vertol deice system detector was mounted on the aircraft nose in front of the copilot windshield (FS 24.5, left BL 18, WL 150) (discussed in app B). The instrumentation Rosemount detector was mounted in front of the right gunner window (FS 85, right BL 46, WL 150) (photo 3). The instrumentation Rosemount detector was connected to a cockpit control panel. A block diagram of the detector operation is shown in figure 1.

**Photo 3. Ice Detector Installation.**

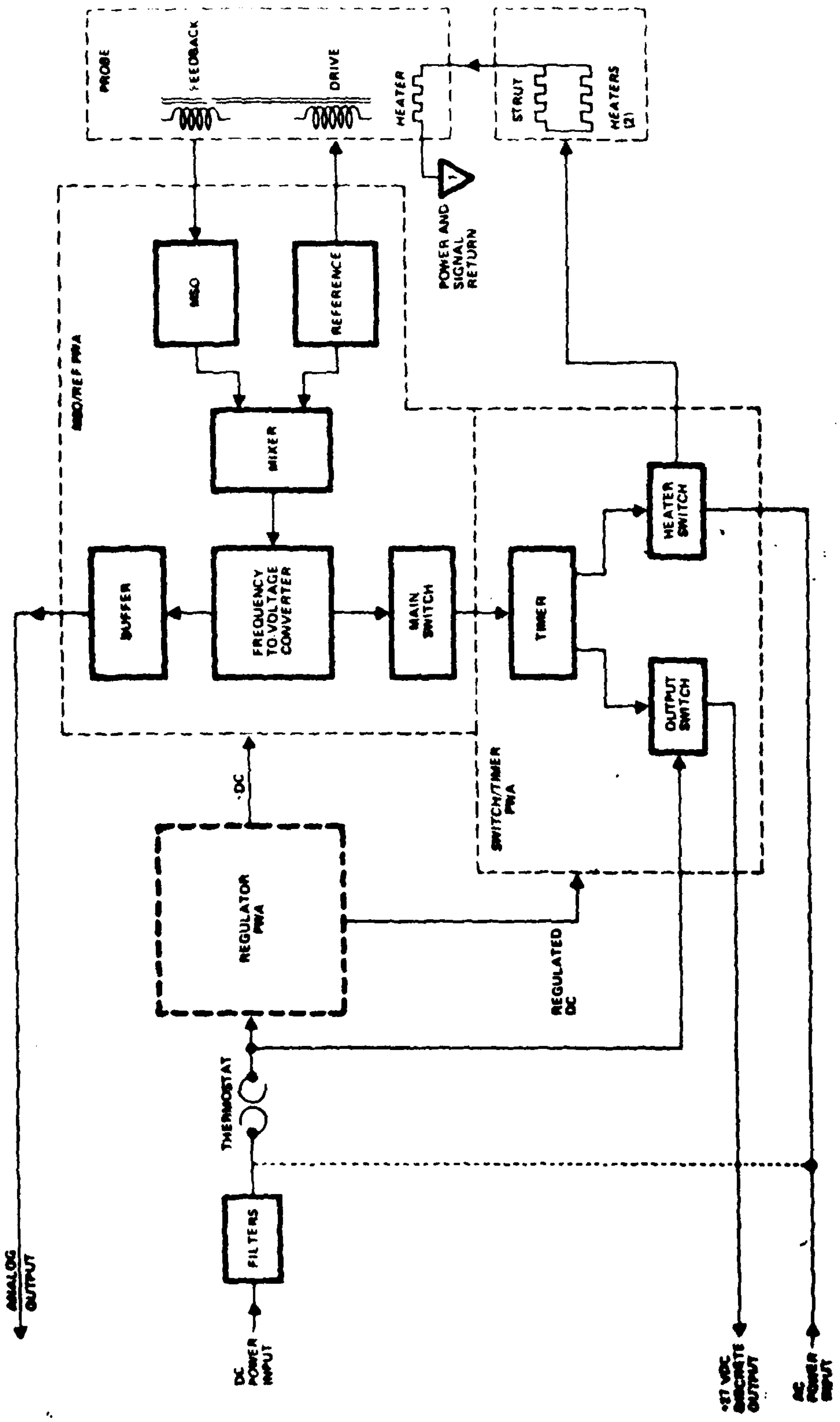


Figure 1. Rosemount Model 871FA Schematic.

11. The operation of the two detectors is identical. The sensing *element of the* ice detector is an axially vibrating probe whose natural frequency changes with ice accumulation. Probe vi' ·ation is achieved with the magnetostrictive oscillator (MSO). The reference os...ator signal is summed with the signal from the MSO to produce a difference frequency (the output of the mixer). The frequency-to-voltage converter changes the difference frequency to a voltage, and when this voltage rea·hes a preset value corresponding to the accumulation of 0.020 inch (0.5mm) of ice, an output signal is provided to the timer. The timer initiates the probe heating cycle which purges the probe of the accumulated ice. A constant-voltage output signal is provided which the Boeing Vertol deice system uses to trigger the control unit (para 9, app B). The signal from the Rosemount detector illuminates a red light on the cockpit control panel and is recorded on magnetic tape. After the probe heating cycle is completed the probe is ready to accrete ice and the sequence is repeated.

12. The frequency-to-voltage converter of the MSO also provides a variable-voltage analog output corresponding to ice thickness. The Rosemount detector signal was differentiated and displayed in the cockpit as an icing severity on the Rosemount Model 512P icing rate meter (photo 4). The Boeing Vertol detector analog output was recorded on magnetic tape for data analysis purposes.

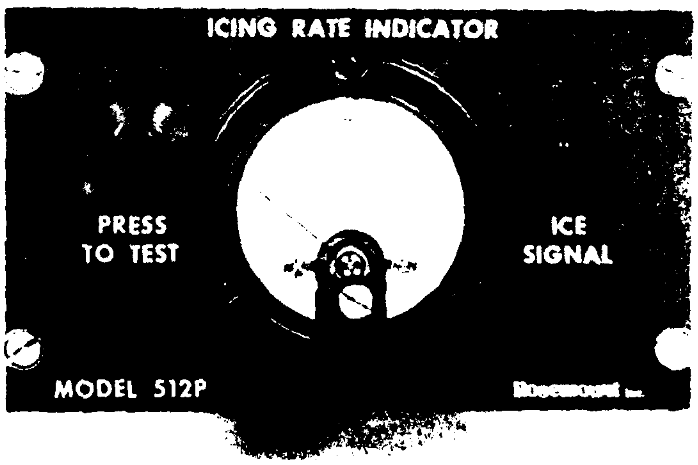


**Photo 4. Special Equipment (Rosemount) Ice Detector Indicator Panel.**

13. The press-to-test button on the cockpit panel was provided to check system operation. Depressing and holding the button creates a difference frequency which simulates ice accumulation on the probe. Proper system operation is indicated by illumination of the red light and deflection of the icing severity needle.

**Normalair-Garrett Ice Detector:**

14. The Normalair-Garrett ice detector is an inferential-type detector. Unlike the Rosemount detector, which allows ice to accrete on a probe, the Garrett senses the amount of free water in the atmosphere. Specifically, the system measures the impingement rate of supercooled liquid water and icing surface temperature. The system consists of three major components: moisture sensing head, control module, and icing severity indicator.

15. The Normalair-Garrett moisture sensing head was mounted on the test aircraft above the Rosemount detector probe (photo 3). The water and skin temperature sensing head consists of two cylindrical heater/sensor probes mounted on a short airfoil section mast. The front heater is exposed directly to the airflow and impinging water droplets. A cross-section view of the moisture sensing head is shown in figure 2. The rear heater is housed within the inertia separator, which prevents any water droplets impinging on its surface. Both heaters are maintained at a constant electrical temperature by the electronic control module. The physical properties of the two probes and the recovery factor of the inertia separator give equal cooling to the two probes under dry air conditions. Therefore, the same electrical power is required to make the temperature of the two probes equal. When supercooled water droplets are present, an increase in power is required by the front probe to maintain equality of temperature with the rear probe. The difference in power levels between the front and rear probes is therefore a fraction of the amount of water evaporated from the front probe in unit time. This power difference is processed by the electronic control module and presented on the cockpit indicator (photo 5) in terms of liquid water content (gm/m$^3$).

16. The icing surface temperature is obtained indirectly by a temperature sensor, which is part of the servo control system, maintaining the sensing head support mast at a temperature set above 0°C. This temperature signal is used to inhibit the indicator at that skin temperature at which no ice can form.

17. In order to check the complete system for correct functioning, a self-test facility is provided on the cockpit panel. When the self-test switch is activated, an electrical imbalance of the front probe temperature is created, which simulates cooling of the probe by water droplets. At the same time, the temperature sensor cut-out is disconnected to allow the check to be carried out in above freezing conditions. The resulting icing severity indicator deflection and warning lamp illumination indicate that both the sensing head and the control circuits are operational. Additionally, a facility is incorporated in the cockpit panel which provides illumination of a warning lamp when a predetermined scale reading is exceeded.

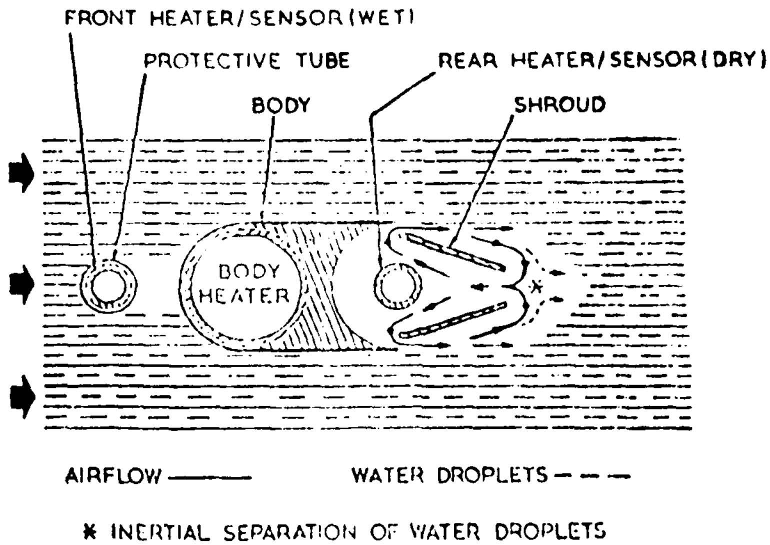


Figure 2. Cross-Section View of Normalair-Garrett Moisture Sensing Head.

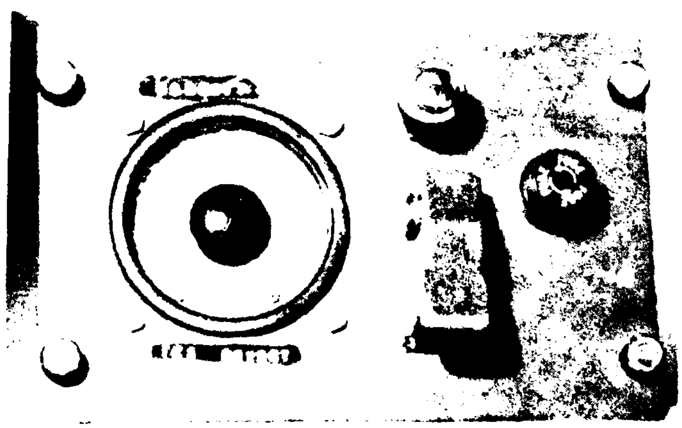

Photo 5. Special Equipment (Normalair-Garrett) Ice Detector Indicator Panel.

**Visual Ice Accretion Probe:**

18. A USAAEFA-designed and fabricated visual ice accretion probe was installed on the copilot door below the window (photo 6). This probe consisted of a 3.5-inch-wide airfoil section rigidly mounted on a support shaft. A 1.75-inch-long rod extended forward from the leading edge of the airfoil section and was marked in 1/4-inch increments. Using this probe, the rate and thickness of ice accretion was observed by the copilot during icing test flights.

**Telemetry and Data Reduction System**

19. A portable telemetry monitoring (TM) and data reduction system was fabricated to allow on-site data analysis. It consisted of the following equipment:

Nems-Clarke Type R10376 solid state TM receiver
EMR-Schlumberger Model 720 PCM bit synchronizer
EMR-Schlumberger Model 2731 PCM frame synchronizer
EMR-Schlumberger Model 713 programmable word selector
Hewlett-Packard Model 5245L electronic counter
Hewlett-Packard Model 4204A oscillator
Tektronix Type 422 oscilloscope
Ampex Model PR 2200 tape transport
Clevite Model 9200 datum time code translator
Gould Model 260 brush recorders (2 each)
EMR-Schlumberger Model 4150 proportional bandwidth subcarrier discrimanator (12 each)
EMR-Schlumberger Model 4150 constant bandwidth subcarrier discriminator (12 each)
Bell and Howell datagraph Model 5-134 oscillograph

20. The TM receiver had a line-of-sight range of approximately 20 to 30 nautical miles and monitored signals on a 1435- to 1540-MHz band. The system converted these signals into a real time display of 12 PCM data channels on the brush recorders and 6 FM data channels on the oscillograph. The channels monitored during a flight were chosen by the project engineer from among any of the channels being recorded by the airborne magnetic tape system. The channels displayed could be changed at any time during the flight.

21. The package allowed for postflight strip-out of the flight tape. Each time the flight tape was run through the system 12 PCM and 6 FM channels could be processed. The electronic counter allowed actual PCM data counts to be compared with pen movements. The flight tape could be rerun until all desired data channels were stripped out. The system allowed for a tape search for a specified time slice and a digital display of the data.

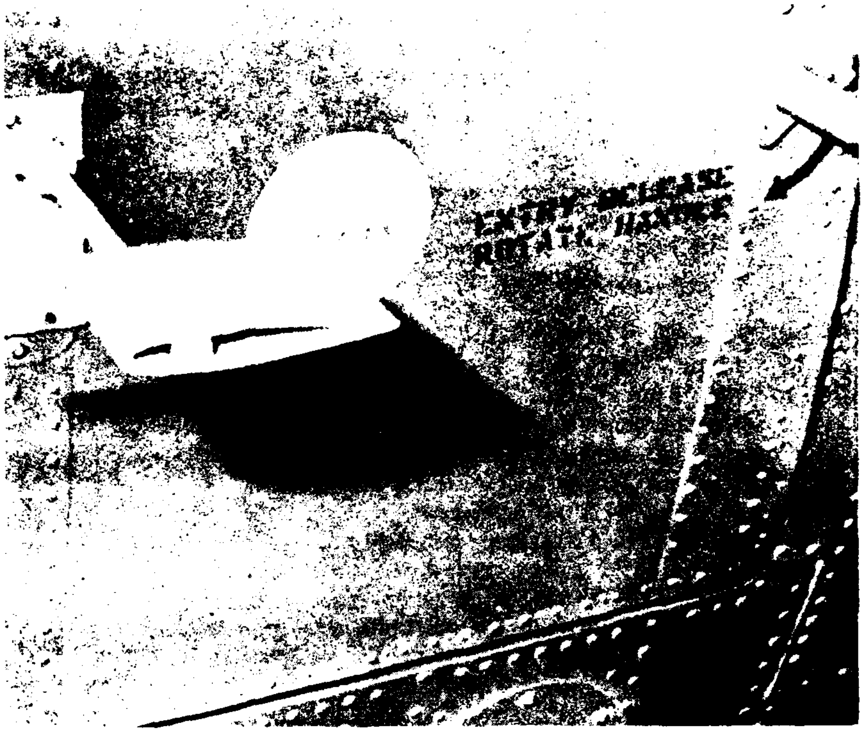

Photo 6. Visual Ice Accretion Probe.

# APPENDIX E. TEST TECHNIQUES AND DATA ANALYSIS METHODS

## TEST TECHNIQUES

### Flight Technique

1. The tests were executed in two phases, using the HISS to generate a spray cloud. The heated blade phase was conducted at six combinations of temperature and LWC with the main rotor, tail rotor, and horizontal stabilizer deice systems activated. The unheated blade phase involved testing at one temperature and LWC combination with the main rotor, tail rotor, and horizontal stabilizer deicing system not activated. The cabin heat, windshield anti-ice, pitot-static system heat, and engine anti-ice were operational for all cloud immersions during both phases.

2. The general test sequence was similar during each phase. Table 1 presents the test matrix of static air temperatures and LWC's used for the heated blade phase. The test approach was to start at the warmest temperature and lowest LWC and progressively build up to colder temperatures and higher LWC's. At each test condition the test aircraft entered the cloud and remained immersed for a predetermined time period or until the HISS water was depleted, the longer immersion times being associated with the lower LWC's. The test condition for the unheated blade phase was -10°C and 0.25 $gm/m^3$ LWC. Immersion time during this phase was based on thickness of ice accretion on the visual ice accretion probe.

Table 1. Test Matrix.

| Temperature (°C) | Liquid Water Content ($gm/m^3$) | | |
|---|---|---|---|
| | 0.25 | 0.50 | 0.75 |
| -5 | X | X | X |
| -10 | X | X | — |
| -15 | X | -- | — |

3. At each test temperature, an engine stall check was conducted. The engine stall check was performed with the engine inlet anti-ice ON and cabin heater ON. From a stable level flight condition, the appropriate ECL was rapidly retarded to START/IDLE. The ECL was then rapidly advanced back to FLT after the engine had stabilized at idle. Testing continued if there were no stalls. Prior to each cloud immersion, level flight performance data at 90 KTAS were obtained with the deice/anti-ice systems ON and OFF.

4. The test aircraft entered the cloud from a position below and 200 feet behind the HISS. Stand-off distance information was provided by a rear-facing radar altimeter mounted on the HISS. After the immersion time had elapsed, the aircraft exited the cloud to document the ice accretion and perform specific engineering tests. Level flight performance data at 90 KTAS were obtained with the deice/anti-ice systems ON. If ice had accreted on the main or tail rotor blades, an autorotation was conducted to determine rotor speed degradation. The aircraft then returned to Fort Wainwright for postflight ice accretion measurements. Subsequent flights were flown at either the same temperature and a higher LWC or at a colder temperature and the lowest untested LWC.

5. During the unheated blade phase, no attempt was made by the pilot to induce main rotor blade shedding. The primary reason was to avoid producing an asymmetrical shed.

## HISS Flow Rate Calculation Method

6. Water flow rate of the HISS, to establish the desired icing severity level for each test flight, was determined using the following technique. The CH-47C spray aircraft used installed calibrated instruments to establish airspeed, altitude, and static air temperature for the desired test condition. The frost point was obtained by utilizing a Cambridge thermoelectric dew-point hygrometer. The frost point was then converted to a dew point using table 2, which was furnished by the instrument manufacturer.

Saturation vapor pressure (millibars) for the dew point and static air temperature was obtained from table 3.

Relative humidity was then computed using the values obtained from table 2 and equation 1:

$$Rh = \frac{P_{VS}}{P_W} \times 100 \qquad (1)$$

Table 2. Cambridge Thermoelectric Dew Point Hygrometer Conversion Values (Degrees Centigrade).

| Frost Point | Dew Point | Frost Point | Dew Point | Frost Point | Dew Point | Frost Point | Dew Point |
|---|---|---|---|---|---|---|---|
| -0.0 | -0.1 | -6.5 | -7.3 | -13.0 | -14.5 | -19.5 | -21.1 |
| -0.5 | -0.7 | -7.0 | -7.9 | -13.5 | -15.0 | -20.0 | -22.2 |
| -1.0 | -1.2 | -7.5 | -8.4 | -14.0 | -15.6 | -20.5 | -22.8 |
| -1.5 | -1.8 | -8.0 | -9.0 | -14.5 | -16.2 | -21.0 | -23.3 |
| -2.0 | -2.3 | -8.5 | -9.5 | -15.0 | -16.7 | -21.5 | -23.9 |
| -2.5 | -2.9 | -9.0 | -10.1 | -15.5 | -17.3 | -22.0 | -24.5 |
| -3.0 | -3.4 | -9.5 | -10.6 | -16.0 | -17.8 | -22.5 | -25.0 |
| -3.5 | -4.0 | -10.0 | -11.2 | -16.5 | -18.4 | -23.0 | -25.6 |
| -4.0 | -4.5 | -10.5 | -11.7 | -17.0 | -18.9 | -23.5 | -26.1 |
| -4.5 | -5.1 | -11.0 | -12.3 | -17.5 | -19.5 | -24.0 | -26.7 |
| -5.0 | -5.6 | -11.5 | -12.8 | -18.0 | -20.0 | -24.5 | -27.2 |
| -5.5 | -6.2 | -12.0 | -13.4 | -18.5 | -20.6 | -25.0 | -27.8 |
| -6.0 | -6.7 | -12.5 | -13.9 | -19.0 | -21.1 | -25.5 | -28.3 |

Table 3. Saturation Vapor Pressure Over Water.
(Millibars)

| Temperature °C | .0 | .1 | .2 | .3 | .4 | .5 | .6 | .7 | .8 | .9 |
|---|---|---|---|---|---|---|---|---|---|---|
| -25 | 0.8070 | 0.799[illegible] | 0.7926 | 0.7854 | 0.7783 | 0.7713 | 0.7643 | 0.7574 | 0.7506 | 0.7438 |
| -24 | 0.8827 | 0.8748 | 0.8671 | 0.8593 | 0.8517 | 0.8441 | 0.8366 | 0.8291 | 0.8217 | 0.8143 |
| -23 | 0.9649 | 0.9564 | 0.9479 | 0.939[illegible] | 0.9314 | 0.9230 | 0.9148 | 0.9067 | 0.8986 | 0.8906 |
| -22 | 1.0538 | 1.0446 | 1.0356 | 1.0264 | 1.0173 | 1.0084 | 0.9995 | 0.9908 | 0.9821 | 0.97[illegible] |
| -21 | 1.1500 | [illegible] | [illegible] | [illegible] | [illegible] | 1.1009 | 1.0913 | 1.0818 | 1.0724 | [illegible] |
| -20 | [illegible] | [illegible] | [illegible] | [illegible] | [illegible] | [illegible] | 1.1906 | 1.1804 | 1.1702 | [illegible] |
| -19 | 1.3666 | [illegible] | [illegible] | [illegible] | [illegible] | 1.3091 | 1.2979 | 1.2868 | 1.2758 | 1.2648 |
| -18 | 1.48[illegible] | 1.4751 | 1.462[illegible] | [illegible] | 1.4381 | 1.4259 | 1.4138 | 1.4018 | 1.3899 | 1.378[illegible] |
| -17 | 1.6186 | [illegible] | [illegible] | [illegible] | [illegible] | 1.5519 | 1.5389 | 1.5259 | 1.5131 | [illegible] |
| -16 | 1.7597 | 1.7451 | 1.7306 | [illegible] | 1.7020 | 1.6879 | 1.6738 | 1.6599 | 1.646[illegible] | [illegible] |
| -15 | 1.9118 | 1.896[illegible] | 1.8805 | [illegible] | [illegible] | 1.8343 | 1.8191 | 1.8041 | 1.7892 | [illegible] |
| -14 | 2.075[illegible] | [illegible] | 2.0418 | [illegible] | 2.0085 | 1.9921 | 1.9758 | [illegible] | 1.9435 | [illegible] |
| -13 | 2.251[illegible] | [illegible] | [illegible] | [illegible] | 2.179[illegible] | 2.1619 | 2.1444 | 2.1270 | 2.1097 | [illegible] |
| -12 | 2.4409 | [illegible] | 2.4016 | [illegible] | [illegible] | 2.3445 | 2.3256 | 2.3069 | 2.2881 | [illegible] |
| -11 | 2.644[illegible] | [illegible] | [illegible] | [illegible] | [illegible] | 2.5408 | [illegible] | 2.5006 | 2.4804 | [illegible] |
| -10 | 2.862[illegible] | [illegible] | [illegible] | [illegible] | [illegible] | 2.7516 | 2.7298 | 2.7082 | 2.6868 | [illegible] |
| -9 | 3.0971 | [illegible] | 3.0480 | [illegible] | [illegible] | 2.9778 | 2.9544 | 2.9313 | 2.9082 | [illegible] |
| -8 | 3.3484 | [illegible] | 3.2967 | [illegible] | 3.2457 | 3.2206 | 3.1955 | 3.1706 | 3.1459 | [illegible] |
| -7 | 3.6177 | 3.5884 | 3.562[illegible] | 3.534[illegible] | 3.5077 | 3.480[illegible] | 3.4539 | 3.4272 | 3.4008 | [illegible] |
| -6 | 3.9061 | [illegible] | [illegible] | [illegible] | [illegible] | 3.7594 | 3.730[illegible] | 3.7023 | 3.6738 | [illegible] |
| [illegible] | 4.2148 | 4.1835 | [illegible] | [illegible] | 4.0888 | 4.0578 | 4.0271 | 3.9966 | 3.966[illegible] | [illegible] |
| [illegible] | [illegible] | [illegible] | [illegible] | [illegible] | [illegible] | 4.3772 | [illegible] | [illegible] | 4.2791 | [illegible] |
| [illegible] | [illegible] | [illegible] | [illegible] | [illegible] | [illegible] | 4.7187 | 4.6834 | 4.6486 | 4.6138 | [illegible] |
| [illegible] | [illegible] | [illegible] | [illegible] | [illegible] | [illegible] | 5.0830 | 5.0446 | 5.0067 | 4.971[illegible] | [illegible] |
| [illegible] | 5.6780 | [illegible] | [illegible] | [illegible] | [illegible] | 5.4736 | 5.4333 | 5.3934 | [illegible] | [illegible] |
| [illegible] | 6.1078 | 6.0630 | 6.0190 | [illegible] | [illegible] | 5.8894 | 5.8466 | 5.8040 | 5.7617 | [illegible] |



FOR OFFICIAL USE ONLY

Where:

$Rh$ = Relative humidity (percent)

$P_{VS}$ = Saturation vapor pressure for dew point (millibars)

$P_W$ = Saturation vapor pressure for static air temperature (millibars)

7. The decay LWC, which is the spray cloud evaporation rate, was then computed using equation 2.

$$LWC_D = \frac{G(100 - Rh)}{4.5G_O} \tag{2}$$

Where:

$LWC_D$ = Decay liquid water content (percent/second)

$G$ = Thermodynamic function (centimeter$^2$/second)

$Rh$ = Relative humidity (percent) (obtained from equation 1)

$G_O$ = $60 \times 10^{-8}$ centimeter$^2$/second (constant)

The value for the thermodynamic function G used in equation 2 was obtained from figure 1 using the static air temperature indicated by the HISS aircraft. Pressure dependence of G is small, so that values for 1000 millibars given in figure 1 were satisfactory for the test altitudes (ref 13, app A).

The programmed LWC based on the desired test condition was then corrected for evaporation using the decay LWC calculated above and equation 3.

$$LWC_C = \left(\frac{LWC_D}{100}\right)\left(\frac{D}{1.6889V_T}\right)(LWC_P) + LWC_P \tag{3}$$

Where:

$LWC_C$ = Corrected liquid water content (gm/m$^3$)

$LWC_D$ = Decay liquid water content (percent/second)

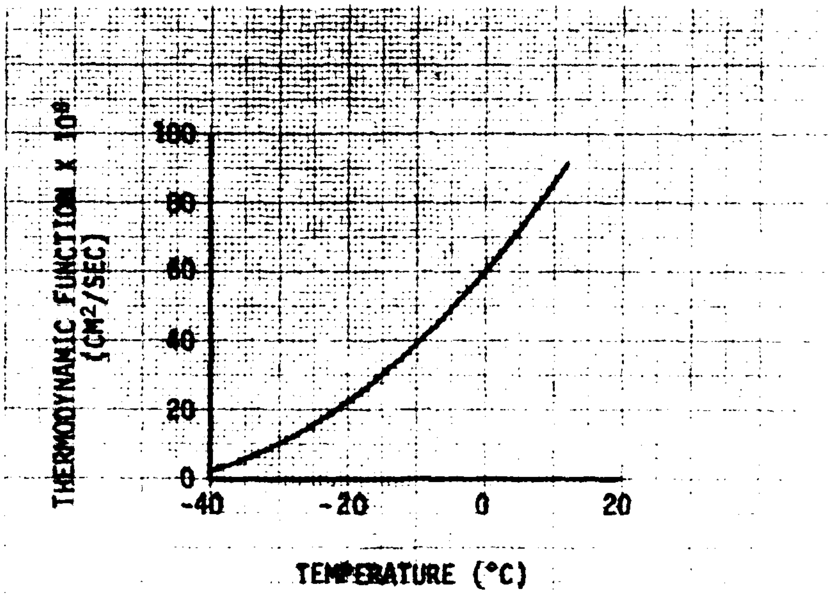


FIGURE I. VARIATION OF THERMODYNAMIC FUNCTION WITH TEMPERATURE AT 1000 MILLIBARS

SOURCE: Byers, H. R., *Elements of Cloud Physics*, Univ of Chicago Press, 1965.

$D$ = 200 feet (constant distance between test and spray aircraft maintained during this test)

1.6889 = Conversion factor (ft/sec/kt)

$V_t$ = 90 knots (constant test airspeed)

$LWC_P$ = Programmed liquid water content (gm/m$^3$)

8. The corrected LWC and figure 3 (ref 14, app A) were then used to determine the required water flow rate. The flow rate obtained from figure 2 and a constant bleed air pressure of 15 pounds per square inch (gauge) were used to establish the spray cloud.

## DATA ANALYSIS METHODS

9. The icing severity was a function of time in the spray cloud, temperature, and LWC. The programmed icing severity was compared with the Rosemount and Garrett ice detectors. Ice accretion was measured in flight using the visual probe and high-speed photography. Additionally, postflight ice accretions were measured immediately upon landing when practicable.

10. Ice shedding characteristics were qualitatively assessed by crewmembers in the test, spray, and chase aircraft. In addition to the high-speed motion pictures taken from the chase and spray aircraft, cameras were mounted on the main and tail rotor blades of the test aircraft. A description of the test aircraft cameras is presented in appendix D. Film obtained from the cameras mounted on the test aircraft did not have sufficient sharpness or clarity to permit an analysis of ice accretion and shedding on the main or tail rotor blades. This was caused by the low ambient light conditions and the unsatisfactory view angles from the location where the cameras were mounted.

11. Vibration levels were qualitatively assessed during each flight. An FM magnetic tape recorder was used to quantify the vibration data. Data obtained from the magnetic tape system were analyzed using a Spectral Dynamics 301 spectral analyzer. The spectral analyzer was used to convert the data from the time domain (acceleration as a function of time) to the frequency domain (acceleration as a function of frequency).

12. Level flight performance degradation due to ice accretion was assessed by comparing the engine power required to maintain constant airspeed and altitude before and after ice accumulation. Shaft horsepower was calculated using equation 4.

$$SHP = N_R \times Q \times K \times \frac{2\pi}{33,000} \tag{4}$$

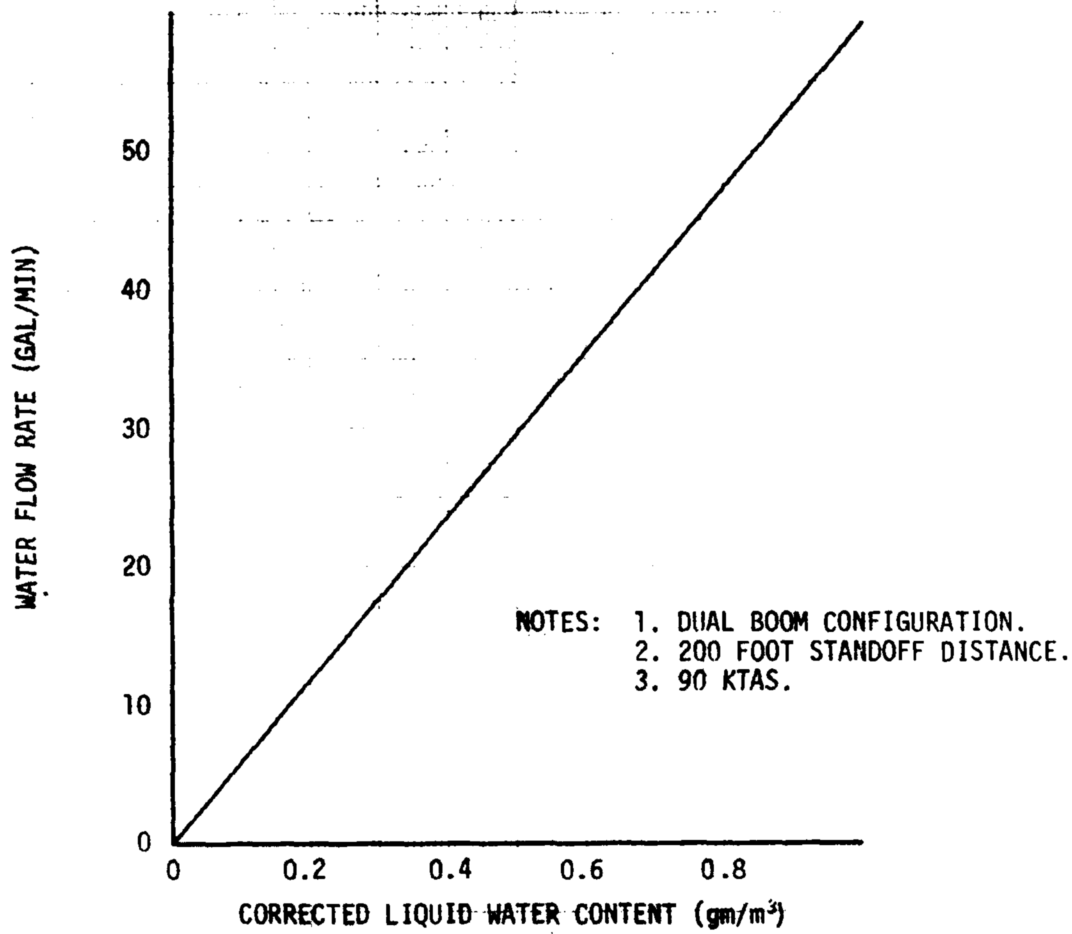


FIGURE 2. WATER FLOW RATE CHART

Where:

SHP = Calculated shaft horsepower (hp)

$N_R$ = Main rotor rotational speed (rev/min)

Q = Engine output shaft torque (ft-lb)

K = Gearing constant between engine and main rotor (67.65)

13. The engine power required to operate the anti-ice/deice systems was also determined by performing engine toppings at various test static air temperatures. The engine topping data were plotted in terms of referred shp versus referred gas temperature ($T_{4.5}$). Referred shp was calculated using equation 5:

$$RSHP = \frac{SHP}{(\delta)(\theta)^{0.5}} \qquad (5)$$

Where:

RSHP = Referred shaft horsepower

SHP = Test shaft horsepower

$\delta = \{1 - (6.875586 \times 10^{-6})(H_P)\}^{5.25585}$

$H_P$ = Test pressure altitude (ft)

$$\theta = \frac{OAT_{static} + 273.15}{288.15}$$

$OAT_{static}$ = Test static air temperature (°C)

14. Autorotational performance degradation due to main and tail rotor ice accretion was evaluated. The collective position required to stabilize at a rotor speed of 300 rpm (105 percent) was measured before and after ice accumulation. The tapeline rates of descent were calculated using equation 6:

$$R/D_{tapeline} = \left(\frac{\Delta H_P}{\Delta t}\right) \frac{T_t}{T_s} \qquad (6)$$

Where:

$R/D_{tapeline}$ = Tapeline rate of descent (ft/min)

$\frac{\Delta Hp}{\Delta t}$ = Change in pressure altitude per given time (ft/min)

$T_t$ = Test ambient air temperature (°K)

$T_s$ = Standard ambient air temperature (°K)

15. The effect of ice accretion on the test aircraft handling qualities was qualitatively assessed by the pilot. An HQRS was used to augment pilot comments and is presented as figure 3. Control positions were quantitatively measured and comparisons made between no-ice base-line data and data recorded after ice accretion.

16. Icing characteristics were described using the following definitions of icing types and severity (ref 15, app A):

a. Icing type definitions:

(1) Rime ice: An opaque granular deposit of ice formed by the rapid freezing of small supercooled water droplets.

(2) Clear ice: A semitransparent smooth deposit of ice formed by the slower freezing of larger supercooled water droplets.

(3) Glime ice: A mixture of clear ice and rime ice.

b. Icing severity definitions:

(1) Trace icing: Ice becomes perceptible. Rate of accumulation slightly greater than rate of sublimation. It is not hazardous even though deicing equipment is not used, unless encountered for an extended period of time (over 1 hour).

(2) Light icing: The rate of accumulation may create a problem if flight is prolonged in this environment (over 1 hour). Occasional use of deicing/anti-icing equipment removes/prevents accumulation. It does not present a problem if the deicing/anti-icing equipment is used.

(3) Moderate icing: The rate of accumulation is such that even short encounters become potentially hazardous and use of deicing/anti-icing equipment or diversion is necessary.

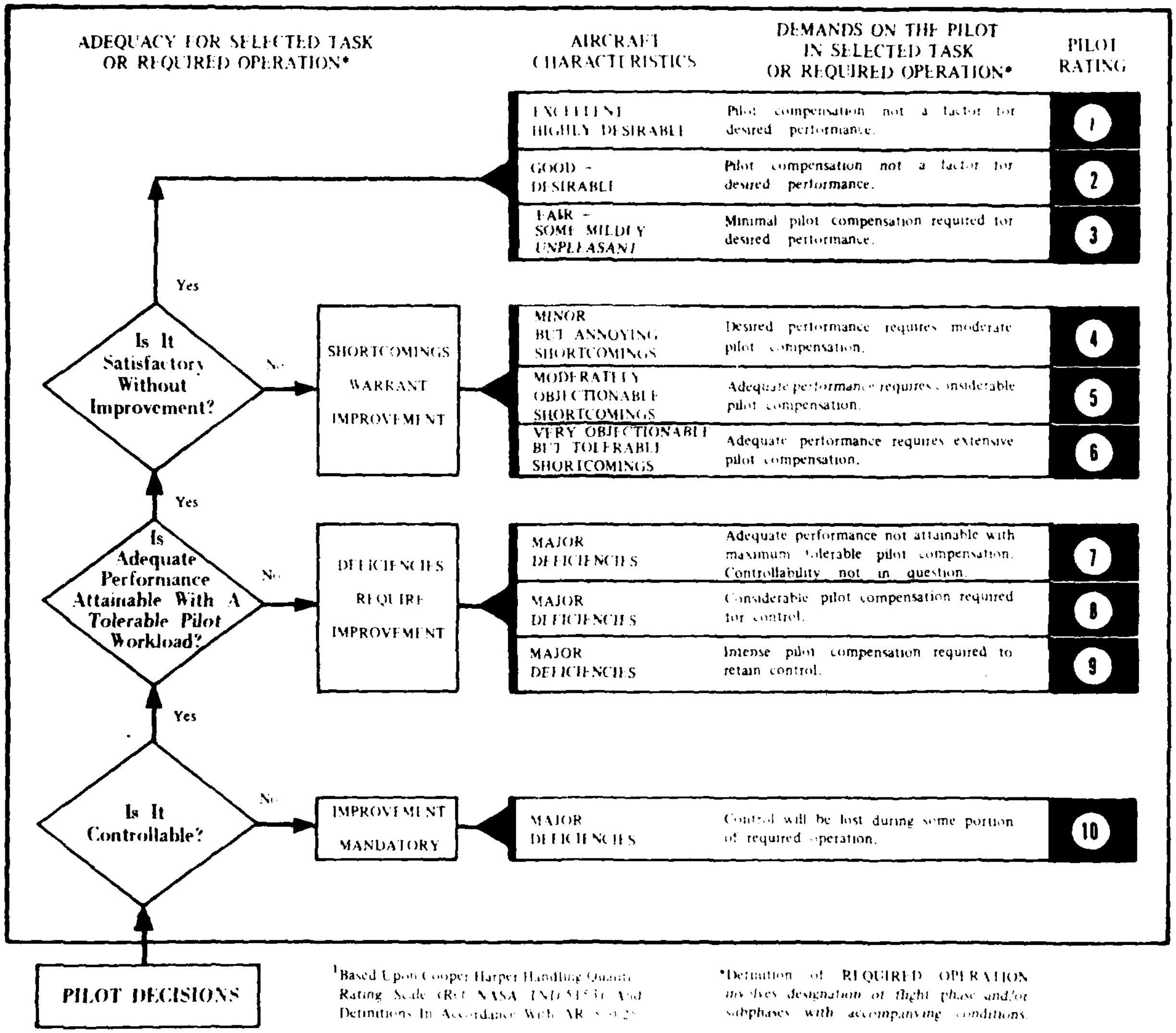


[1]Based Upon Cooper Harper Handling Quality Rating Scale (Ref NASA TN [illegible]) And Definitions In Accordance With AR [illegible]

*Definition of REQUIRED OPERATION involves designation of flight phase and/or subphases with accompanying conditions.

**Figure 3. Handling Qualities Rating Scale**

(4) Severe icing: The rate of accumulation is such that deicing/anti-icing equipment fails to reduce or control the hazard. Immediate diversion is necessary.

17. Results were categorized as deficiencies or shortcomings in accordance with the following definitions (ref 16, app A):

Deficiency: A defect or malfunction discovered during the life cycle of an equipment that constitutes a safety hazard to personnel; will result in serious damage to the equipment if operation is continued; indicates improper design or other cause of an item or part, which seriously impairs the equipment's operational capability. A deficiency normally disables or immobilizes the equipment; and if occurring during test phases, will serve as a bar to type classification action.

Shortcoming: An imperfection or malfunction occurring during the life cycle of equipment, which should be reported and which must be corrected to increase efficiency and to render the equipment completely serviceable. It will not cause an immediate breakdown, jeopardize safe operation, or materially reduce the usability of the material or end product. If occurring during test phases, the shortcoming should be corrected if it can be done without unduely complicating the item or inducing another undesirable characteristic such as increased cost, weight, etc.

# APPENDIX F. ICING FLIGHT SUMMARIES

Table 1. Icing Flight Summary.
Heated Phase

| Flight No. and Date | Average Static Outside Air Temperature (°C) | Programmed Liquid Water Content ($gm/m^3$) | Average Density Altitude (ft) | Average True Airspeed (kt) | Average Gross Weight (lb) | Average Longitudinal Center of Gravity (in.) |
|---|---|---|---|---|---|---|
| 2<br>9 Oct 76 | -6.5 | 0.25 | 1590 | 86 | 15,580 | 205.6 |

Time in cloud: (hr) Total this flight 0.1 Cumulative total 0.1 Number of deice system cycles Zero Type ice observed: Glime

Postflight Ice Measurements (in.)

| Component | Maximum Ice | Component | Maximum Ice |
|---|---|---|---|
| Chin bubbles | 1/10 | Main rotor hub/deice dome | Zero |
| Windshield wipers | 1/4 | Main rotor pitch change links | Zero |
| Aircraft nose | 1/10 | Pendulum absorbers | Zero |
| Eyebrow windows | Zero | Main rotor blades | Zero |
| Pilot/copilot windshields | Zero | Hub cap | Zero |
| Center windshield | 1/8 | Pitot-static tubes | Zero |
| Cockpit doors | Zero | #1 engine inlet/trans fairing | Zero |
| Cockpit steps | 1/4 | #2 engine inlet/trans fairing | Zero |
| Cockpit door windows | Zero | FM antenna | Zero |
| Main landing gear | 1/4 | Horizontal stabilizers | Trace |
| Nose gear | 1/4 | Vertical fin | Zero |
| Rotating beacons | Not recorded | Tail rotor hub and slider | Zero |
| Deice system OAT probe | Zero | Tail rotor blades | Zero |
| Center windshield OAT probe | 1/8 | Upper handholds | Zero |
| Instrumentation OAT probe | 1/10 | Fwd crown work platform supports | Trace |

General comments:

1. Deice system Rosemount ice detector heater failed. This rendered the deice system inoperative.
2. UTTAS exited cloud after 7 minutes due to deice system failure.



FOR OFFICIAL USE ONLY

Table 2. Icing Flight Summary.
Heated Phase

| Flight No. and Date | Average Static Outside Air Temperature (°C) | Programmed Liquid Water Content (gm/m3) | Average Density Altitude (ft) | Average True Airspeed (kt) | Average Gross Weight (lb) | Average Longitudinal Center of Gravity (in.) |
|---|---|---|---|---|---|---|
| 4<br>12 Oct 76 | -11.5 | 0.25 | -270 | 88 | 15,860 | 296.8 |

Time in cloud: (hr) Total this flight 0.2 Cumulative total 0.3 Number of deice system cycles 1 Type ice observed: Glime

Postflight Ice Measurements (in.)

| Component | Maximum Ice | Component | Maximum Ice |
|---|---|---|---|
| Chin bubbles | 1/4 | Main rotor hub/deice dome | Trace |
| Windshield wipers | 3/8 | Main rotor pitch change links | Trace |
| Aircraft nose | 3/8 | Pendulum absorbers | Trace |
| Eyebrow windows | Zero | Main rotor blades | 1/16 |
| Pilot/copilot windshields | Zero | Hub cap | Zero |
| Center windshield | 3/8 | Pitot-static tubes | Zero |
| Cockpit doors | Zero | #1 engine inlet/trans fairing | Zero |
| Cockpit steps | Not recorded | #2 engine inlet/trans fairing | 1/4 |
| Cockpit door windows | Zero | FM antenna | Zero |
| Main landing gear | 1/4 | Horizontal stabilizers | Trace |
| Nose gear | 1/4 | Vertical fin | Zero |
| Rotating beacons | Not recorded | Tail rotor hub and slider | Zero |
| Deice system OAT probe | Not recorded | Tail rotor blades | Zero |
| Center windshield OAT probe | Not recorded | Upper handholds | Not recorded |
| Instrumentation OAT probe | Not recorded | Fwd crown work platform supports | 1/4 |

General comments:

1. The HISS lower spray bar was not operational.
2. UTTAS exited cloud after 10 minutes due to inadequate spray cloud thickness.
3. Instrumentation Rosemount ice detector indicated M to H after UTTAS exited cloud.

Table 3. Icing Flight Summary.
Heated Phase

| Flight No. and Date | Average Static Outside Air Temperature (°C) | Programmed Liquid Water Content ($gm/m^3$) | Average Density Altitude (ft) | Average True Airspeed (kt) | Average Gross Weight (lb) | Average Longitudinal Center of Gravity (in.) |
|---|---|---|---|---|---|---|
| 5 13 Oct 76 | -6.5 | 0.50 | 2640 | 84 | 15,800 | 206.5 |

Time in cloud: (hr) Total this flight 0.4 Cumulative total 0.7 Number of deice system cycles 14 Type ice observed: Glime

Postflight Ice Measurements (in.)

| Component | Maximum Ice | Component | Maximum Ice |
|---|---|---|---|
| Chin bubbles | 3/8 | Main rotor hub/deice dome | 3/8 |
| Windshield wipers | 1/2 | Main rotor pitch change links | 1/16 |
| Aircraft nose | 3/8 | Pendulum absorbers | 1/4 |
| Eyebrow windows | Zero | Main rotor blades | Zero |
| Pilot/copilot windshields | Zero | Hub cap | 3/16 |
| Center windshield | 3/8 | Pitot-static tubes | 1/2 |
| Cockpit doors (hinge) | 3/4 | #1 engine inlet/trans fairing | Zero |
| Cockpit steps | 7/8 | #2 engine inlet/trans fairing | Zero |
| Cockpit door windows | Zero | FM antenna | Zero |
| Main landing gear | 1/8 | Horizontal stabilizers | 1/8 |
| Nose gear | 1/2 | Vertical fin | Trace |
| Rotating beacons | Not recorded | Tail rotor hub and slider | Zero |
| Deice system OAT probe | Not recorded | Tail rotor blades | Zero |
| Center windshield OAT probe | 1/2 | Upper handholds | 1/4 |
| Instrumentation OAT probe | Not recorded | Fwd crown work platform supports | 1/4 |

General comments:

1. Normalair-Garrett ice detector indicated 0.5 to 2 $gm/m^3$ and averaged 0.7 to 0.8 $gm/m^3$.
2. Rosemount indicated H.

Table 4. Icing Flight Summary.
Heated Phase

| Flight No. and Date | Average Static Outside Air Temperature (°C) | Programmed Liquid Water Content (gm/m3) | Average Density Altitude (ft) | Average True Airspeed (kt) | Average Gross Weight (lb) | Average Longitudinal Center of Gravity (in.) |
|---|---|---|---|---|---|---|
| 6 15 Oct 76 | -11.0 | 0.25 | 6400 | 90 | 15,760 | 206.3 |

Time in cloud: (hr) Total this flight 0.6 Cumulative total 1.3

Number of deice system cycles 9

Type ice observed: Glime

**Postflight Ice Measurements (in.)**

| Component | Maximum Ice | Component | Maximum Ice |
|---|---|---|---|
| Chin bubbles | 3/4 | Main rotor hub/deice dome | 1/8 |
| Windshield wipers | 1-3/8 | Main rotor pitch change links | 1/8 |
| Aircraft nose | 3/4 | Pendulum absorbers | Zero |
| Eyebrow windows | Zero | Main rotor blades (swan neck) | 1/4 |
| Pilot/copilot windshields | Zero | Hub cap | 1/8 |
| Center windshield | 3/4 | Pitot-static tubes | Zero |
| Cockpit doors | 1/2 | #1 engine inlet/trans fairing | Zero |
| Cockpit steps | 1/4 | #2 engine inlet/trans fairing | Zero |
| Cockpit door windows | Zero | FM antenna | Zero |
| Main landing gear | Zero | Horizontal stabilizers | 3/8 |
| Nose gear | Zero | Vertical fin | 1/4 |
| Rotating beacons | 1/8 | Tail rotor hub and slider | Trace |
| Deice system OAT probe | Zero | Tail rotor blades | Zero |
| Center windshield OAT probe | Zero | Upper handholds | Not recorded |
| Instrumentation OAT probe | Zero | Fwd crown work platform supports | Not recorded |

General comments:

1. Postflight ice measurements were accomplished with OAT above freezing.
2. Normalair-Garrett and Rosemount ice detectors agreed with programmed values.
3. Cabin heater inlet iced over. Air deflector installed forward of the inlet.

Table 5. Icing Flight Summary.
Heated Phase

| Flight No. and Date | Average Static Outside Air Temperature (°C) | Programmed Liquid Water Content ($gm/m^3$) | Average Density Altitude (ft) | Average True Airspeed (kt) | Average Gross Weight (lb) | Average Longitudinal Center of Gravity (in.) |
|---|---|---|---|---|---|---|
| 7<br>16 Oct 76 | -6.0 | 0.75 | 6260 | 92 | 15,740 | 206.2 |

**Time in cloud:** (hr) **Total this flight** 0.2 **Cumulative total** 1.5 **Number of deice system cycles** 8 **Type ice observed: Glime**

**Postflight Ice Measurements (in.)**

| Component | Maximum Ice | Component | Maximum Ice |
|---|---|---|---|
| Chin bubbles | Zero | Main rotor hub/deice dome | 1/4 |
| Windshield wipers | 1/2 | Main rotor pitch change links | Trace |
| Aircraft nose | 3/4 | Pendulum absorbers | Zero |
| Eyebrow windows | Zero | Main rotor blades | Zero |
| Pilot/copilot windshields | Zero | Hub cap | 1/4 |
| Center windshield | 1/4 | Pitot-static tubes | Zero |
| Cockpit doors | Runback | #1 engine inlet/trans fairing | Zero |
| Cockpit steps | 7/16 | #2 engine inlet/trans fairing | 1/2 |
| Cockpit door windows | Zero | FM antenna | Zero |
| Main landing gear | Zero | Horizontal stabilizers | 1/4 |
| Nose gear | Zero | Vertical fin | 1/8 |
| Rotating beacons | Zero | Tail rotor hub and slider | Zero |
| Deice system OAT probe | Zero | Tail rotor blades | Zero |
| Center windshield OAT probe | Not recorded | Upper handholds | 1/2 |
| Instrumentation OAT probe | Zero | Fwd crown work platform supports | 1/4 |

General comments:

1. Postflight ice measurements were accomplished with OAT above freezing.
2. Normalair-Garrett and Rosemount indications were erratic.
3. Switching transient data obtained.
4. Engine toppings accomplished.

Table 6. Icing Flight Summary.
Heated Phase

| Flight No. and Date | Average Static Outside Air Temperature (°C) | Programmed Liquid Water Content ($gm/m^3$) | Average Density Altitude (ft) | Average True Airspeed (kt) | Average Gross Weight (lb) | Average Longitudinal Center of Gravity (in.) |
|---|---|---|---|---|---|---|
| 9<br>28 Oct 76 | -16.5 | 0.25 | -1580 | 88 | 15,640 | 205.8 |

Time in cloud: (hr) Total this flight 0.8 Cumulative total 2.3 Number of deice system cycles 9 Type ice observed: Glime

Postflight Ice Measurements (in.)

| Component | Maximum Ice | Component | Maximum Ice |
|---|---|---|---|
| Chin bubbles | 5/8 | Main rotor hub/deice dome | 1/8 |
| Windshield wipers | 3/16 | Main rotor pitch change links | 1/8 |
| Aircraft nose | 3/16 | Pendulum absorbers | 1/2 |
| Eyebrow windows | Zero | Main rotor blades (swan neck) | 1/2 |
| Pilot/copilot windshields | Zero | Hub cap | 1/8 |
| Center windshield | 2-1/4 | Pitot-static tubes | 1-1/4 |
| Cockpit doors | Runback | #1 engine inlet/trans fairing | Zero |
| Cockpit steps | 1-1/8 | #2 engine inlet/trans fairing | 1/2 |
| Cockpit door windows | Zero | FM antenna | Zero |
| Main landing gear | 1/16 | Horizontal stabilizers | 3/4 |
| Nose gear | 3/4 | Vertical fin | 1/8 |
| Rotating beacons | Trace | Tail rotor hub and slider | Zero |
| Deice system OAT probe | Zero | Tail rotor blades | 1/8 |
| Center windshield OAT probe | Not recorded | Upper handholds | Not recorded |
| Instrumentation OAT probe | Zero | Fwd crown work platform supports | Not recorded |

General comments:

1. ROTOR DEICE caution light illuminated momentarily after 37 minutes immersion. Condition corrected and the UTTAS reentered the cloud.
2. Normalair-Garrett and Rosemount indications agreed with the programmed values.

Table 7. Icing Flight Summary.
Heated Phase

| Flight No. and Date | Average Static Outside Air Temperature (°C) | Programmed Liquid Water Content (gm/m3) | Average Density Altitude (ft) | Average True Airspeed (kt) | Average Gross Weight (lb) | Average Longitudinal Center of Gravity (in.) |
|---|---|---|---|---|---|---|
| 10 29 Oct 76 | -13.0 | 0.50 | 1300 | 87 | 15,720 | 206.2 |

Time in cloud: (hr) Total this flight 0.5 Cumulative total 2.8 Number of deice system cycles 17 Type ice observed: Glime

Postflight Ice Measurements (in.)

| Component | Maximum Ice | Component | Maximum Ice |
|---|---|---|---|
| Chin bubbles | 1-5/8 | Main rotor hub/deice dome | 1/4 |
| Windshield wipers | 11/16 | Main rotor pitch change links | 1/4 |
| Aircraft nose | 2 | Pendulum absorbers | 1 |
| Eyebrow windows | 3 | Main rotor blades (swan neck) | 1/2 |
| Pilot/copilot windshields | Zero | Hub cap | 1/4 |
| Center windshield | 2 | Pitot-static tubes | 1-7/8 |
| Cockpit doors (hinges) | 1-1/2 | #1 engine inlet/trans fairing | Zero |
| Cockpit steps | 1-1/2 | #2 engine inlet/trans fairing | 1 |
| Cockpit door windows | 1/8 | FM antenna | Zero |
| Main landing gear | 1/8 | Horizontal stabilizers | 1/2 |
| Nose gear | 1-3/4 | Vertical fin | 1/4 |
| Rotating beacons | Trace | Tail rotor hub and slider | Zero |
| Deice system OAT probe | Trace | Tail rotor blades | Zero |
| Center windshield OAT probe | 1-3/4 | Upper handholds | 3/4 |
| Instrumentation OAT probe | 1-3/4 | Fwd crown work platform supports | 1-1/2 |

General comments:

1. Pre- and postcloud autorotation accomplished with no significant degradation in performance.
2. Erratic and inaccurate airspeed indications in level and climbing flight.
3. Normalair-Garrett and Rosemount ice detectors indicated higher than programmed.
4. Left side of lower spray bar inoperative.

Table 8. Icing Flight Summary.
Unheated Phase

| Flight No. and Date | Average Static Outside Air Temperature (°C) | Programmed Liquid Water Content ($gm/m^3$) | Average Density Altitude (ft) | Average True Airspeed (kt) | Average Gross Weight (lb) | Average Longitudinal Center of Gravity (in.) |
|---|---|---|---|---|---|---|
| 11<br>30 Oct 76 | -12.5 | 0.25 | -620 | 89 | 15,980 | 207.3 |

**Time in cloud:** (hr) **Total this flight** 0.1 **Cumulative total** 2.9 **Number of deice system cycles** Zero **Type ice observed: Glime**

**Postflight Ice Measurements (in.)**

| Component | Maximum Ice | Component | Maximum Ice |
|---|---|---|---|
| Chin bubbles | 1/8 | Main rotor hub/deice dome | 1/8 |
| Windshield wipers | 1/4 | Main rotor pitch change links | 1/8 |
| Aircraft nose | 1/4 | Pendulum absorbers | 1/8 |
| Eyebrow windows | Zero | Main rotor blades | 1/16 |
| Pilot/copilot windshields | Zero | Hub cap | 1/8 |
| Center windshield | 1/8 | Pitot-static tubes | 1/4 |
| Cockpit doors | Zero | #1 engine inlet/trans fairing | Zero |
| Cockpit steps | 3/8 | #2 engine inlet/trans fairing | 1/8 |
| Cockpit door windows | Zero | FM antenna | Zero |
| Main landing gear | Zero | Horizontal stabilizers | 1/8 |
| Nose gear | 1/8 | Vertical fin | Not recorded |
| Rotating beacons | Trace | Tail rotor hub and slider | Not recorded |
| Deice system OAT probe | Zero | Tail rotor blades | Not recorded |
| Center windshield OAT probe | Not recorded | Upper handholds | Not recorded |
| Instrumentation OAT probe | Not recorded | Fwd crown work platform supports | Zero |

General comments:

1. UTTAS remained in cloud until 1/4 inch of ice was observed on visual probe.
2. No significant power required or autorotational performance degradation.

Table 9. Icing Flight Summary.
Unheated Phase

| Flight No. and Date | Average Static Outside Air Temperature (°C) | Programmed Liquid Water Content (gm/m$^3$) | Average Density Altitude (ft) | Average True Airspeed (kt) | Average Gross Weight (lb) | Average Longitudinal Center of Gravity (in.) |
|---|---|---|---|---|---|---|
| 12 1 Nov 76 | -13.5 | 0.25 | -740 | 89 | 15,860 | 206.8 |

Time in cloud: (hr) Total this flight 0.3 Cumulative total 3.2

Number of deice system cycles Zero

Type ice observed: Glime

Postflight Ice Measurements (in.)

| Component | Maximum Ice | Component | Maximum Ice |
|---|---|---|---|
| Chin bubbles | 1/4 | Main rotor hub/deice dome | 3/8 |
| Windshield wipers | 3/8 | Main rotor pitch change links | 3/4 |
| Aircraft nose | 1/4 | Pendulum absorbers | 3/8 |
| Eyebrow windows | Zero | Main rotor blades | 7/8 |
| Pilot/copilot windshields | Zero | Hub cap | 1/4 |
| Center windshield | 3/8 | Pitot-static tubes | Not recorded |
| Cockpit doors | Zero | #1 engine inlet/trans fairing | Zero |
| Cockpit steps | 1/4 | #2 engine inlet/trans fairing | 1/2 |
| Cockpit door windows | Zero | FM antenna | Zero |
| Main landing gear | Zero | Horizontal stabilizers | 1/4 |
| Nose gear | 1/8 | Vertical fin | 1/8 |
| Rotating beacons | 1/8 | Tail rotor hub and slider | Zero |
| Deice system OAT probe | Zero | Tail rotor blades | 1/16 |
| Center windshield OAT probe | Not recorded | Upper handholds | Not recorded |
| Instrumentation OAT probe | Not recorded | Fwd crown work platform supports | 3/4 |

General comments:

1. UTTAS remained in cloud until 1/2 inch of ice was observed on the visual probe.
2. Significant degradation in level flight and autorotational performance was observed.

# APPENDIX G. TEST DATA

FIGURE 1

REFERRED SHAFT HORSEPOWER AND REFERRED MEASURED GAS TEMPERATURE

YUH-60A S/N 73-21658

LEFT ENGINE YT700-GE-700 S/N 207269

| SYMBOL | AVG Hp (FT) | AVG OAT (°C) | ROTOR SPEED (RPM) |
|---|---|---|---|
| ◺ | 2620 | -10.5 | 285 |
| △ | 4520 | -6.0 | 285 |
| △ | 7700 | -10.5 | 285 |
| ◇ | 7100 | -6.0 | 285 |
| □ | 2240 | -16.0 | 286 |
| ○ | 3940 | -11.5 | 286 |

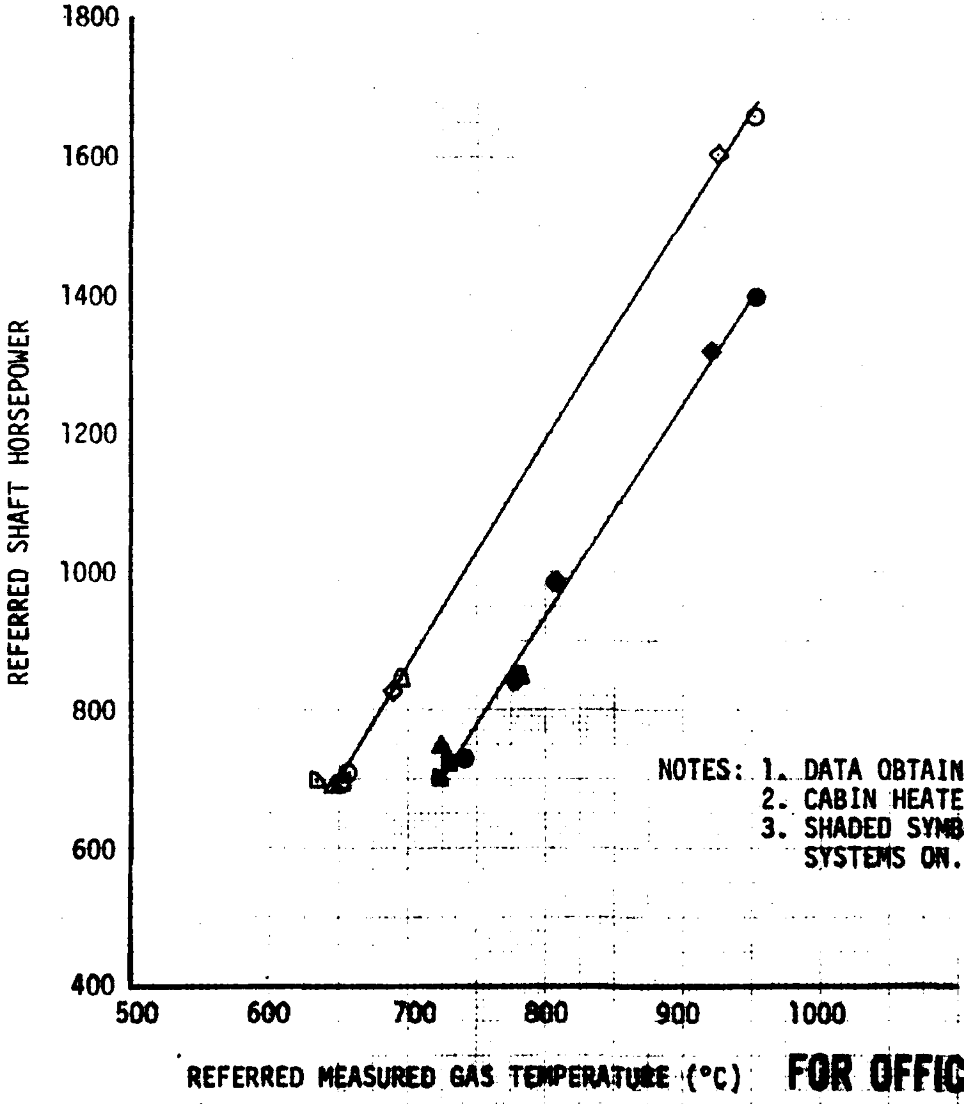


NOTES: 1. DATA OBTAINED IN LEVEL FLIGHT.
2. CABIN HEATER ON.
3. SHADED SYMBOLS DENOTE ANTI-ICE SYSTEMS ON.

**FOR OFFICIAL USE ONLY**

FIGURE 2
REFERRED SHAFT HORSEPOWER AND REFERRED
MEASURED GAS TEMPERATURE
YUH-61A S/N 73-21658
RIGHT ENGINE YT700-GE-700 S/N 207273

| SYMBOL | AVG Hp (FT) | AVG OAT (°C) | ROTOR SPEED (RPM) |
|---|---|---|---|
| ◁ | 2620 | -10.5 | 285 |
| △ | 4520 | -6.0 | 285 |
| △ | 7700 | -10.5 | 285 |
| ◇ | 7100 | -6.0 | 285 |
| □ | 2240 | -16.0 | 286 |
| ○ | 3940 | -11.5 | 286 |

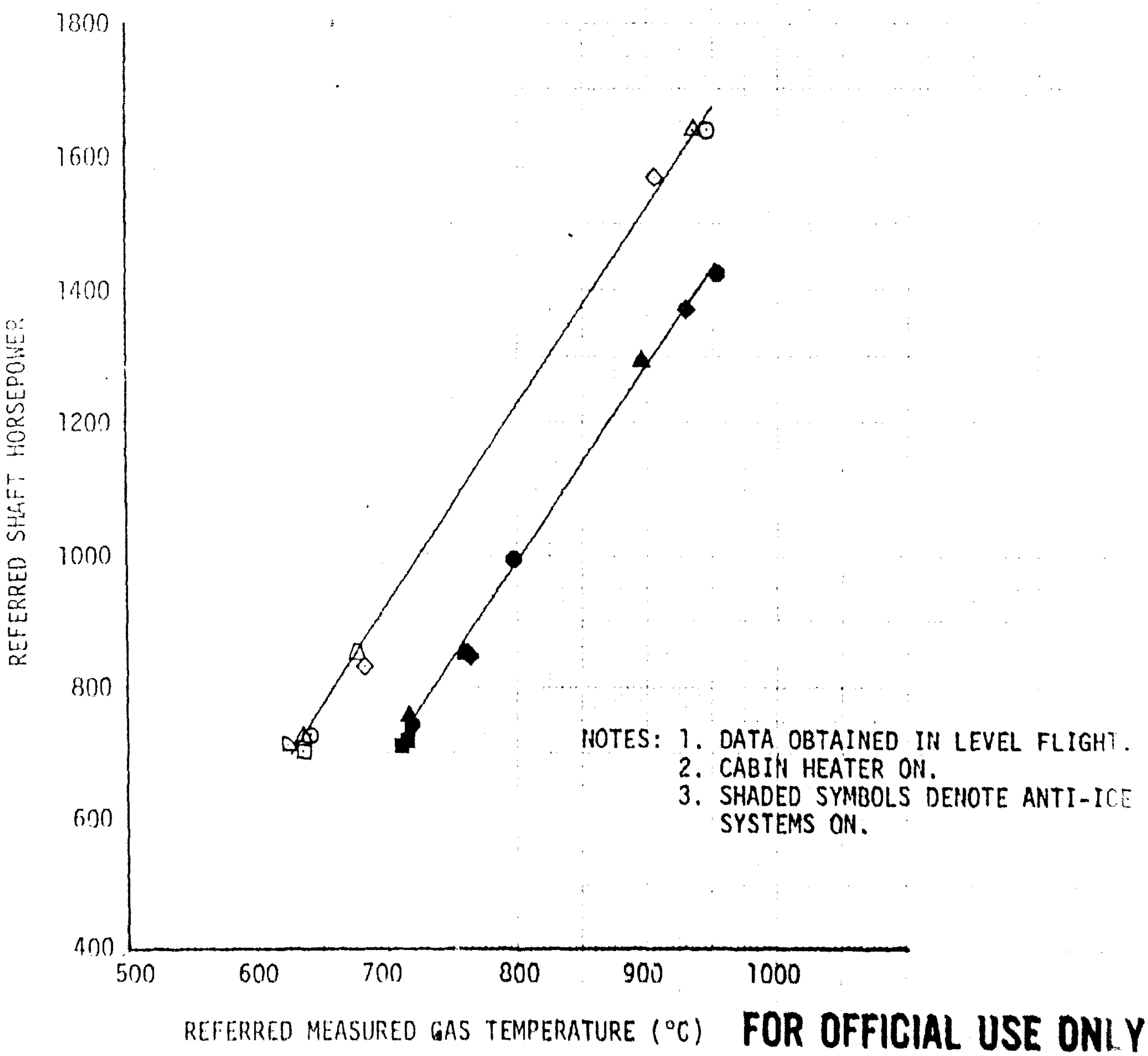


**FOR OFFICIAL USE ONLY**

# APPENDIX H. PHOTOGRAPHS

Photo 1. Engine Nacelle Ice Accretion.

Photo 2. Ice Accretion on Windshield Support Structure.



FOR OFFICIAL USE ONLY

Photo 3. Ice Accretion on Pitot Tube Support Strut.

Photo 4. Pebble Ice Accretion